SOUND PROPAGATION IN STREETS

by

Kangpil Lee
B.S.M.E., Seoul National University
1972

SUBMITTED IN PARTIAL FULFILLMENT
OF THE REQUIREMENTS FOR THE
DEGREE OF MASTER OF
SCIENCE

at the

Massachusetts Institute of Technology

August, 1974

Signature of Author........
Department of Mechanical Engineering
August, 1974

Certified by...
Thesis Supervisor

Accepted by.....
Chairman, Departmental Committee
on Graduate Students

SOUND PROPAGATION IN STREETS

by

Kangpil Lee

Submitted to the Department of Mechanical
Engineering on August 12, 1974 in partial
fulfillment of the requirements for the
degree of Master of Science.

ABSTRACT

Propagation of sound in city streets is investigated
with simplified models. For the low frequency case, an
analytic solution is obtained by means of eigenfunction
expansion of the wave equation in streets and street inter-
sections. For the high frequency case, a simple nomogram
which can predict the sound level in streets is obtained by
using the ray tracing and the image summing technique.
Finally, the ground effect is added to the sound level
obtained from the nomogram.

Thesis Supervisor: Huw G. Davies

Title: Associate Professor
                      Department of Mechanical Engineering

ACKNOWLEDGEMENTS

TABLE OF CONTENTS

4

LIST OF FIGURES

Page

Figure

I. INTRODUCTION

In recent years more and more people are concerned about the ever increasing urban noise level due to various noise sources such as automobiles, subways, aircrafts or industrial plants. In order to find a proper measure to reduce the noise level, it is necessary to understand the sound propagation phenomena, to begin with.

A large number of studies have been dedicated to the problem which is related to sound propagation in urban environs. Schlatter [1] looked at the problem of a point source inside a semi-confined space, using the idea of image source, and incoherent varying strength line source approximation. Davies [2] solved the problem of sound propagation in corridors using a form of geometrical approach, whose result includes the propagation at junctions and corners.

Wiener, Malme, Gogos [3], and Delaney, Copeland, Payne [4] conducted the field experiments on urban noise propagation. Delaney, Rennie, and Collins [5] conducted a scale model investigations on traffic noise propagation. Donovan [6] investigated the sound propagation from an elevated noise source such as aircraft, into urban environs with a series of model experiments. Recently, Holmes and Lyon [7] have succeeded in building a numerical model of urban noise propagation using the Monte Carlo Simulation technique [8], which can handle the

8

irregularities of street width.

In most of the above studies, the problems were dealt with case by case, thus lacking the generality and facility in applications. It is the purpose of this study to find a simple design chart or a nomogram that can be used to easily predict the sound level in streets.

In the first part of this study, the ground effect will be neglected to avoid complexities, however, it will be discussed briefly later in Chapter IV. The low frequency case, in which the wavelength is much greater than the street width, will be studied first. Fig. 1 shows the model which consists of N layers of periodically spaced buildings of rectangular cross-sections with hard walls, and the streets of uniform width, with a plane wave incident on it.

Previous work of this kind can be found in Kristiansen and Fahy [9], where the same problem was solved by eigenfunction expansion of the wave equation inside the streets. His method ended up with an infinite number of simultaneous equations which can be solved approximately only by computer. Shenderov [10] solved the problem of 1 layer of periodically spaced scatterers using a slot impedance method. The former method with some modification is chosen to find an analytic solution to the low frequency case. Also, the insertion loss at a junction of streets will be estimated by applying the continuity

of pressure and volume velocity at the junction.

In the high frequency case, the model will be a part of the previous one shown in Fig. 2. Since the plane wave mode is not particularly relevant in explaining the physical sound propagation phenomena in streets, a point nomopole source is chosen here. Also, the ray tracing and image summing technique will be used to find the sound field.

The image summing technique has often been used [2, 6, 11, 12, 13] which treats each reflected wave path as coming from an image source [14], and has been proved by experiment to be adequate to predict the sound level in high frequency case.

By using the above techniques, a general purpose computer program is written which can calculate the sound pressure level in a straight street with N side streets or in the Nth side street where N = 0, 1, 2, ... An intensive effort is given to find the suitable non-dimensional variables which will enable us to simplify the huge amount of data produced by the computer program mentioned above. By using the idea of averaging, or spreading the intensity of a sound beam ·over the street width, it is possible to find those non-dimensional variables which can be used to draw a simple nomogram to predict the sound level in streets.

Finally, the neglected ground effect will be included.
A number of studies have been dedicated to this problem.
Moore [15] looked at the problem of a free acoustic field
from a point source which has pure tone or multiple tones, with
the presence of a ground surface. He included the effect of
source directivity, and the size of the source. Delaney and
Bazely [16] studied the effect of ground upon the aircraft
noise measurement using a fibrous absorbent material for his
model. Piercy and Embleton [17], and Sutherland [18] treated
the sound propagation problem near the ground level which can
be applied to vehicle noise measurements. Recently, Bettis and
Sexton [19] conducted vehicle passby measurements and compared
the result with the theoretical prediction which was obtained,
from a broad band source, integrating over the frequency range
considered.

All the above studies on ground effect were about open
field propagation. To include the ground effect to the street
propagation problem where we have two parallel walls, the method
used by Bettis and Sexton [19] will be applied with some
modifications. A white noise of 100 Hz to 8000 Hz will be used
as an input sound, which is A-weighted according to the center
frequency of one third octave band.

The result of this ground effect will be combined with
the result from the nomogram giving the desired noise level in
streets.
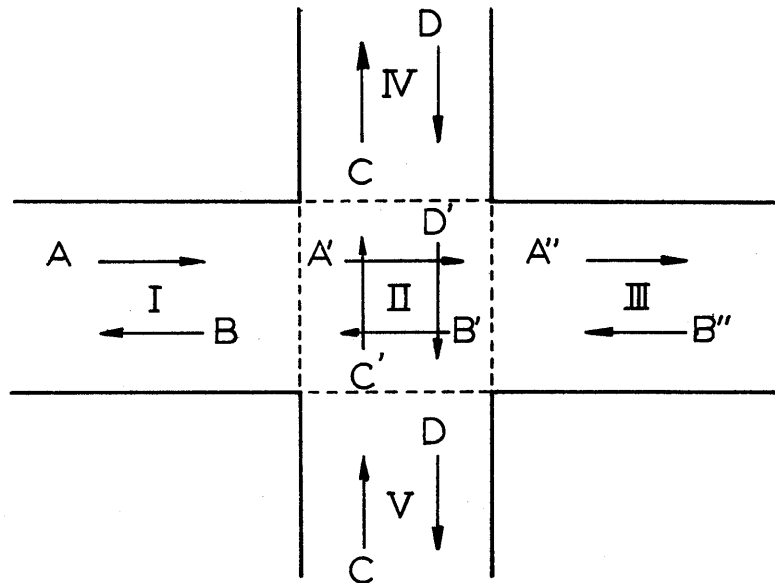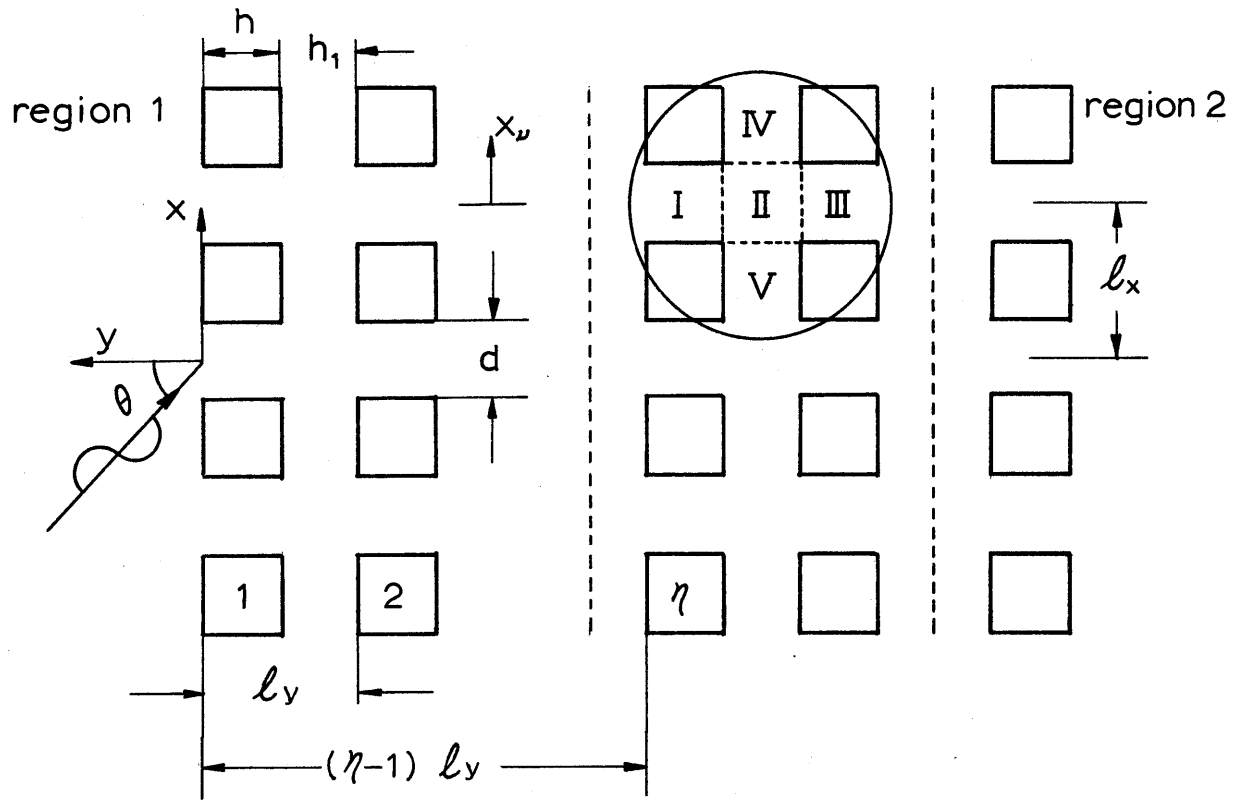
Fig. 1 Model of Streets for Low Frequency
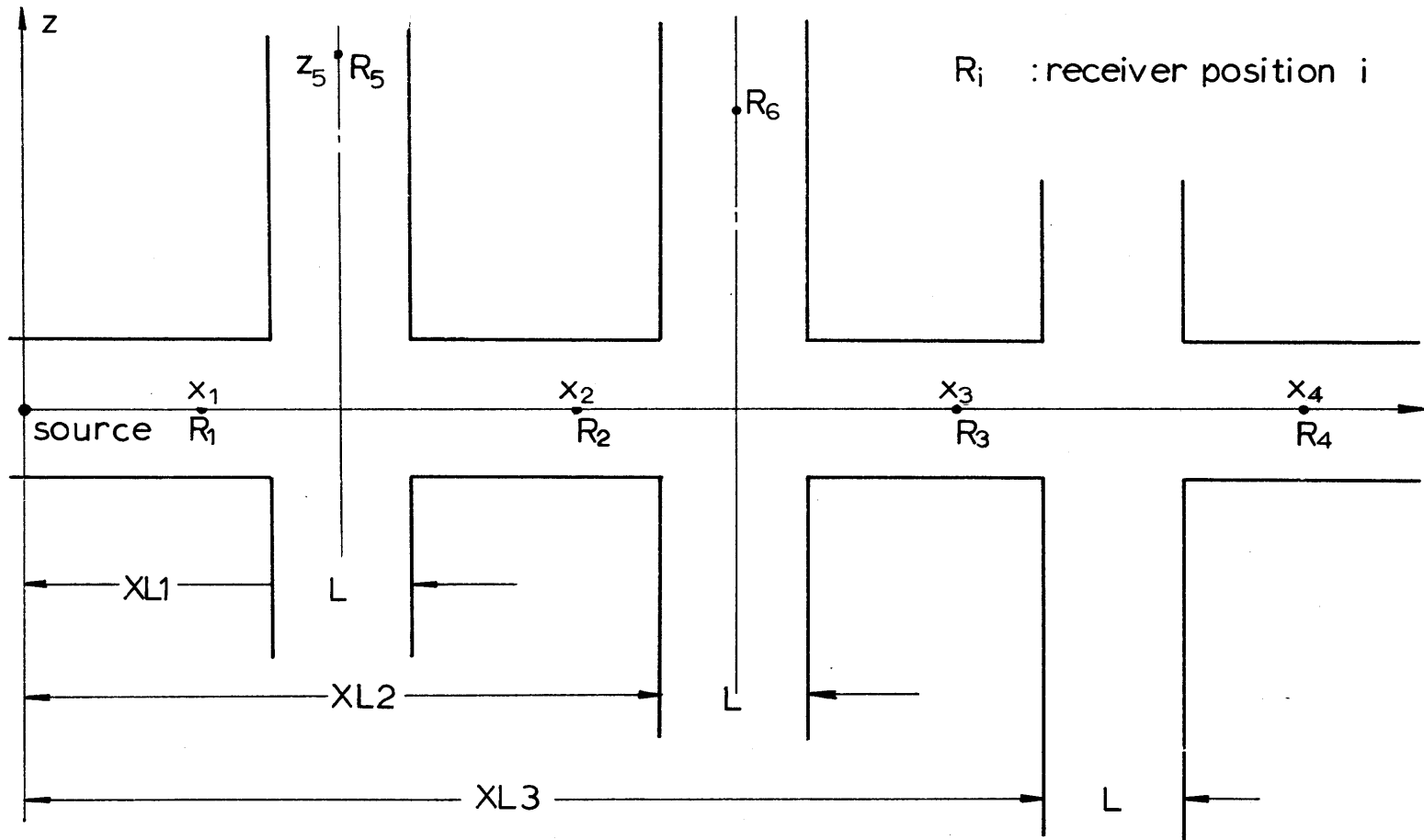
Fig. 2   Model of Streets for High Frequency

II. LOW FREQUENCY SOLUTION

A. Periodic Arrays

The same approach that Kristiansen and Fahy [9] used will be used to solve the low frequency case. While they solved the problem numerically, here, an analytic solution will be obtained in very low frequency region in which the wavelength is much greater than the street width d or h, i.e. kd << 1, kh_1 << 1.

A plane wave with unit amplitude is incident on the arrays of buildings which will be called scatterers hereafter, with the angle of incidence θ. The surfaces of scatterers are smooth, flat and rigid with reflection coefficient of 1. The ground effect will be neglected and we are looking at the problem on z = constant plane, thus making the problem two dimensional. We wish to solve for the sound field in the slots of the periodic array and for the fields reflected and transmitted by the array.

In Fig. 1 the pressure field in region 1, which is composed of the incident and the reflected waves, is given by

$$\Phi_1 = e^{j(\alpha_0 x + \beta_0 y)} + \sum_{r=-\infty}^{r=\infty} R_r e^{j(\alpha_r x - \beta_r y)} \tag{1}$$

and the pressure field in region 2 which is composed of transmitted waves, is given by

$$\Phi_2 = \sum_{r=-\infty}^{r=\infty} T_r \; e^{j[\alpha_r x + \beta_r (N-1)\ell_y]} \tag{2}$$

where R_r and T_r are the amplitudes of the reflected and transmitted waves respectively, and

$$\alpha_r = \alpha_0 + 2\pi r/\ell_x$$

$$\beta_r = (k^2 - \alpha_r^2)^{1/2} \qquad \text{for } k^2 > \alpha_r^2$$

$$= -j(\alpha_r^2 - k^2)^{1/2} \qquad \text{for } k^2 < \alpha_r^2$$

The pressure field for the streets, which will be called slots hereafter, can be found by solving the wave equation by separation of variables and imposing the hard wall boundary conditions. For the slot intersections, the pressure fields are the super-position of two slot fields normal to each other. Due to the periodicity in x-direction, the pressure field along the x direction will differ in phase only for fixed y. Therefore, by solving for the νth slot, we can extend the result to the whole region applying Floquet's theorem [20] which can be expressed as

$$\Phi(x_\nu + \nu \ell_x, y) = e^{j\alpha_0 \nu \ell_x} \; \Phi(x_\nu, y) \tag{3}$$

Since we are dealing with the low frequency case in which the slot width is much smaller than the wavelength, we can

assume that only plane waves are propagating inside the slots
and slot intersections. Thus, the pressure field in region I
of Fig. 1 is given by

$$\Phi_I = e^{j\alpha_o \nu \ell_x} (A\, e^{jk(y+(\eta-1)\ell_y)} + B\, e^{-jk(y+(\eta-1)\ell_y)})$$

(4)

where A and B are the amplitudes of the plane waves travelling
in the right or left hand directions respectively. Similar
expressions can be written for the regions II, III, IV, V
using the amplitudes A', B', C, D, C', D', A", B".

Applying pressure and particle velocity continuity at
the interfaces for each two adjacent columns of scatterers from
column 1 and 2, to column N-1, and N, we can eliminate all the
amplitudes except the amplitudes A, B of the first column, and
the amplitudes A", B" of the Nth column, which have the relations

$$\begin{vmatrix} A''_N \\ B''_N \end{vmatrix} = \begin{vmatrix} f & g \\ f' & g' \end{vmatrix} \begin{vmatrix} A \\ B \end{vmatrix}$$

(5)

where the elements f, g, f', g' of the transfer matrix are given
in Appendix.

The next step is to equate the acoustic pressure and
particle velocity over the entry surface of the first column and
the exit surface of the Nth column which results in the following
relations among A, B, A''_N, B''_N, R_r and T_r.

$$w_o + \sum_r R_r w_r = A + B \qquad (6)$$

$$\beta_o \ell \, \delta(\alpha_o - \alpha_s) - \beta_s R_s \ell_x = kd[A - B] \, w_s \qquad (7)$$

$$\sum_r T_r w_r = e^{-jkh} A_N'' + e^{jkh} B_N'' \qquad (8)$$

$$\beta_s T_s = kd \, w_s [e^{-jkh} A_N'' - e^{jkh} B_N''] \qquad (9)$$

where

$$w_r = \frac{\sin(\alpha_r d/2)}{\alpha_r d/2}$$

$$\beta_s = (k^2 - \alpha_r^2)^{1/2} \qquad \text{for} \quad k^2 > \alpha_r^2$$

$$= -j(\alpha_r^2 - k^2)^{1/2} \qquad \text{for} \quad k^2 < \alpha_r^2$$

By eliminating A, B, A_N'', B_N'' from equations (5), (6), (7) (8), (9), two infinite sets of linear simultaneous equations are obtained.

$$R_s + g_1 T_s = \frac{\beta_o}{\beta_s} \delta(s) + g_2 \frac{kd}{\ell_x} \frac{w_s}{\beta_s} \sum_r T_r w_r \qquad (10)$$

$$g_3 T_s = \frac{kd \, w_o}{\ell_x} \frac{w_s}{\beta_s} + \frac{kd \, w_s}{\ell_x \beta_s} \sum [R_r w_r + g_4 T_r w_r] \qquad (11)$$

where the coefficients g_1, g_2, etc., are given in Appendix. By multiplying w_s, and summing over s from $-\infty$ to $+\infty$, equations (10), (11) can be rewritten in terms of $\widetilde{R}$, $\widetilde{T}$,

17

$$\widetilde{R} + g_1 \widetilde{T} = c_1 + c_3 g_2 \widetilde{T} \tag{12}$$

$$g_3 \widetilde{T} = c_2 + c_3 \widetilde{R} + c_3 g_4 \widetilde{T} \tag{13}$$

where
$$\widetilde{R} = \sum_s R_s w_s$$

$$\widetilde{T} = \sum_s w_s T_s$$

$$c_1 = w_o \ , \qquad c_2 = \frac{kd \ w_o}{\ell_x} \sum_s \frac{w_s^2}{\beta_s^2} \ , \qquad c_3 = c_2/w_o$$

$\widetilde{R}$, $\widetilde{T}$ are solved from equations (12), (13) and substituted into equations (10), (11), giving the desired amplitudes R_s and T_s for the N scatterer case:

$$R_s = \delta(s) - kd \ (\frac{2w_o}{\ell_x} \frac{g_1}{g_3} \frac{w_s}{\beta_s}) + O \ (kd)^2 \tag{14}$$

$$T_s = kd \ (\frac{2w_o}{\ell_x} \frac{1}{g_3} \frac{w_s}{\beta_s}) + O \ (kd)^2 \tag{15}$$

In a special case where there is only one column of scatterers as shown in Fig. 3a , R_s and T_s have a simple form as,

$$R_s = \delta(s) + kd \ \frac{2w_o}{\ell_x} \frac{w_s}{\beta_s} \frac{1 + \xi_1^2}{1 - 2\xi_2^2 + \xi_1^2} + O \ (kd)^2 \tag{16}$$

$$T_s = kd \ \frac{-4w_o}{\ell_x} \frac{w_s}{\beta_s} \frac{\xi_1}{\xi_1^2 - 2\xi_2 + 1} + O \ (kd)^2 \tag{17}$$

where $\xi_1 = e^{-jkh}$, $\xi_2 = e^{jkh}$

Several other special cases can be derived. When the width of the scatterer, h, becomes much smaller than the wavelength, thus forming the shape of slits in a thin plate, (Fig. 3b), R_s and T_s can be expressed as

$$R_s \cong \delta(s) + j \frac{2dw_o}{h\ell_x} \frac{w_s}{\beta_s} \tag{18}$$

$$T_s \cong j \frac{-2dw_o}{h\ell_x} \frac{w_s}{\beta_s} \tag{19}$$

Another special case is shown in Fig. 3c , which is the problem of scattering by sets of narrow strips of width d. According to Babinet's principle [21], the sum of the wave diffracted from one boundary and the wave diffracted from the inverse boundary is just the undistorted plane wave. By applying above principle, we can get the amplitudes R_s, T_s of the strip scattering problem from equations (18), (19) which are shown below

$$R_s \cong j \frac{-2dw_o}{h\ell_x} \frac{w_s}{\beta_s} \tag{20}$$

$$T_s \cong \delta(s) + j \frac{2dw_o}{h\ell_x} \frac{w_s}{\beta_s} \tag{21}$$

Equations (20),(21) may be useful for the problem of scattering
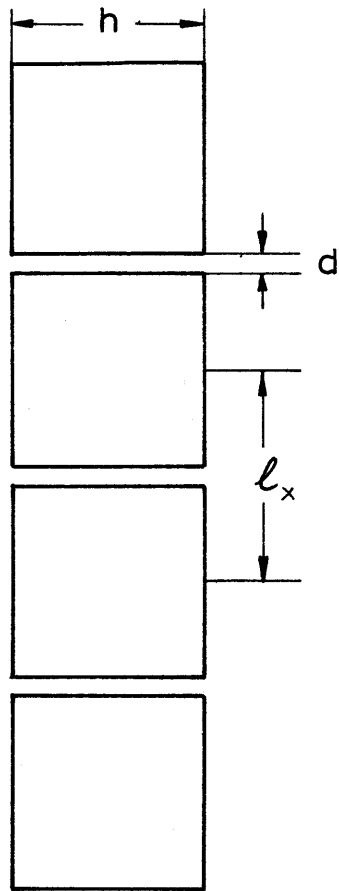
Fig. 3a

1-Column Scatterer
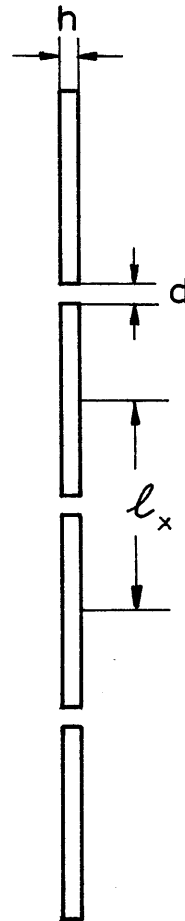
Fig. 3b

Slits in a Thin Plate
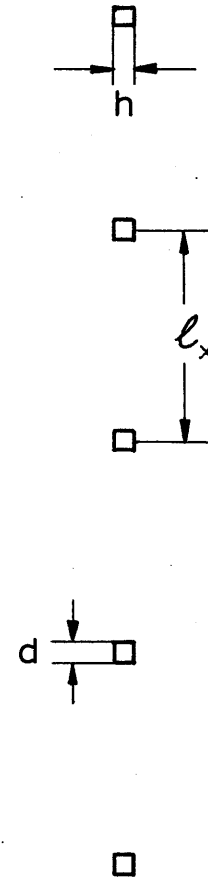
Fig. 3c

Narrow Strips

by trees.

B. Insertion Loss Due to an Intersection

      In this section, the influence of the side streets on
the transmission of the sound waves in a street will be assessed.
The presence of the side street causes a change in acoustic
impedance at the intersection, so that a reflected wave is
produced. A part of the incident wave will go to the side
street which has the input acoustic impedance Z_s. The power loss
due to above two phenomena will be estimated.
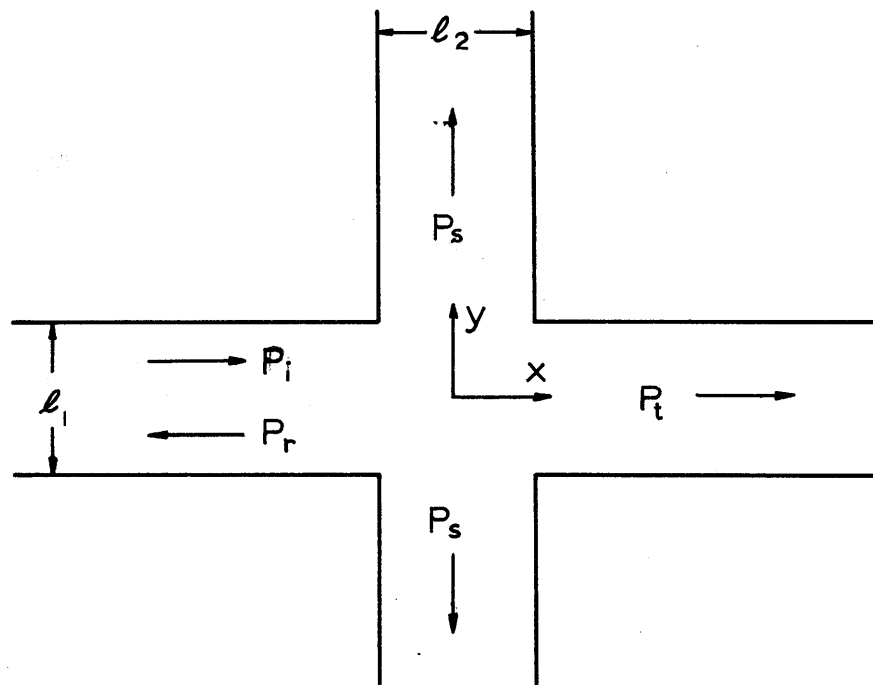
Fig. 4 Waves at an Intersection

The incident plane wave P_i is given by

$$P_i = A_i e^{j(\omega t - kx)} \tag{22}$$

The reflected wave P_r , transmitted wave P_t can be expressed as

$$P_r = A_r e^{j(\omega t + kx)} \tag{23}$$

$$P_t = A_t e^{j(\omega t - kx)} \tag{24}$$

Choosing the center of intersection as an origin

$$P_i = A_i e^{j\omega t}$$

$$P_r = A_r e^{j\omega t} \tag{25}$$

$$P_t = A_t e^{j\omega t}$$

Similarly, the pressure at the center of intersection due to the wave transmitted into the side branch can be expressed as

$$P_s = A_s e^{j\omega t} \tag{26}$$

From the continuity of pressure at the origin,

$$P_i + P_r = P_t = P_s \tag{27}$$

Assuming $Z_s = \rho_0 c/s_2$, the volume velocities in this region are given by

22

$$U_i = \frac{P_i}{\rho_0 c/s_1} \ , \qquad U_r = -\frac{P_r}{\rho_0 c/s_1}$$

(28)

$$U_t = \frac{P_t}{\rho_0 c/s_1} \qquad U_s = \frac{P_s}{\rho_0 c/s_2}$$

where $s_1 = \ell_1 \cdot$ unit height

$s_2 = \ell_2 \cdot$ unit height

and for simplicity, $\ell_1 = \ell_2 = \ell$.

From the continuity of volume velocity,

$$U_i + U_r = U_t + 2 U_s$$

(29)

Solving equations (27), (29) we get the following relations.

$$A_r = -\frac{1}{2} A_i \ , \quad A_t = \frac{1}{2} A_i \ , \quad A_s = \frac{1}{2} A_i$$

(30)

The ratio of the power transmitted into the straight street and the side street beyond the intersection to the incident power are given by

$$\frac{Power_t}{Power_i} = \frac{|A_t|^2}{|A_i|^2} = \frac{1}{4}$$

(31)

$$\frac{Power_s}{Power_i} = \frac{|A_s|^2}{|A_i|^2} = \frac{1}{4}$$

23

Thus, from above result, we can conclude that in a very low frequency case, the power level transmitted through the intersection is 6 dB down from the incident power level.

In general, we expect that the low frequency case has little application to propagation in city streets. The application considered by Kristiansen and Fahy [9] was to the acoustic behavior of nuclear reactor heat exchangers. The results have been included, however, for completeness. And, it is certainly of interest that an intersection provides an appreciable insertion loss of 6 dB at very low frequencies.

III. HIGH FREQUENCY SOLUTION

When a sound wave reflects from a surface, the
Fresnel zone [22] becomes smaller and smaller as the frequency
of the wave increases, and in the limit, it becomes a point
reflection. Therefore, the ray tracing technique can be
used for high frequency waves. By high frequency, it is
meant that the wavelength of the sound wave is much smaller
than the street width.

Here, a part of the previous model is shown in Fig. 2
as the present model.

Several approaches will be used to estimate the sound
pressures at various receiver positions such as 1, 2, 3, etc.
in Fig. 2.

A. Incoherent Line Source Approximation for a Straight Street

This is the case when a receiver is at the position
1 in Fig. 2. In order to have a close look at the problem,
we will treat only a single street as in Fig. 5.

Here, discrete image sources were approximated by a
continuous varying strength line source, so that the net
acoustic power of the line source in each image street is
equivalent to the power of a discrete point image source which
would have occupied the image street.

Fig. 5   Incoherent Varying Strength
Line Source

$\alpha \dfrac{W}{L} \exp(-\mu|z|)$

$\beta' W$

$R^3 W$

$R^2 W$

$R W$

W

$R W$

$R^2 W$

$R^3 W$

W : source power(watts)

R : intensity reflection
coefficient

α : $-(\ln R)/L$

β' : $(1 - R^{.5})/(1 + R^{.5})$
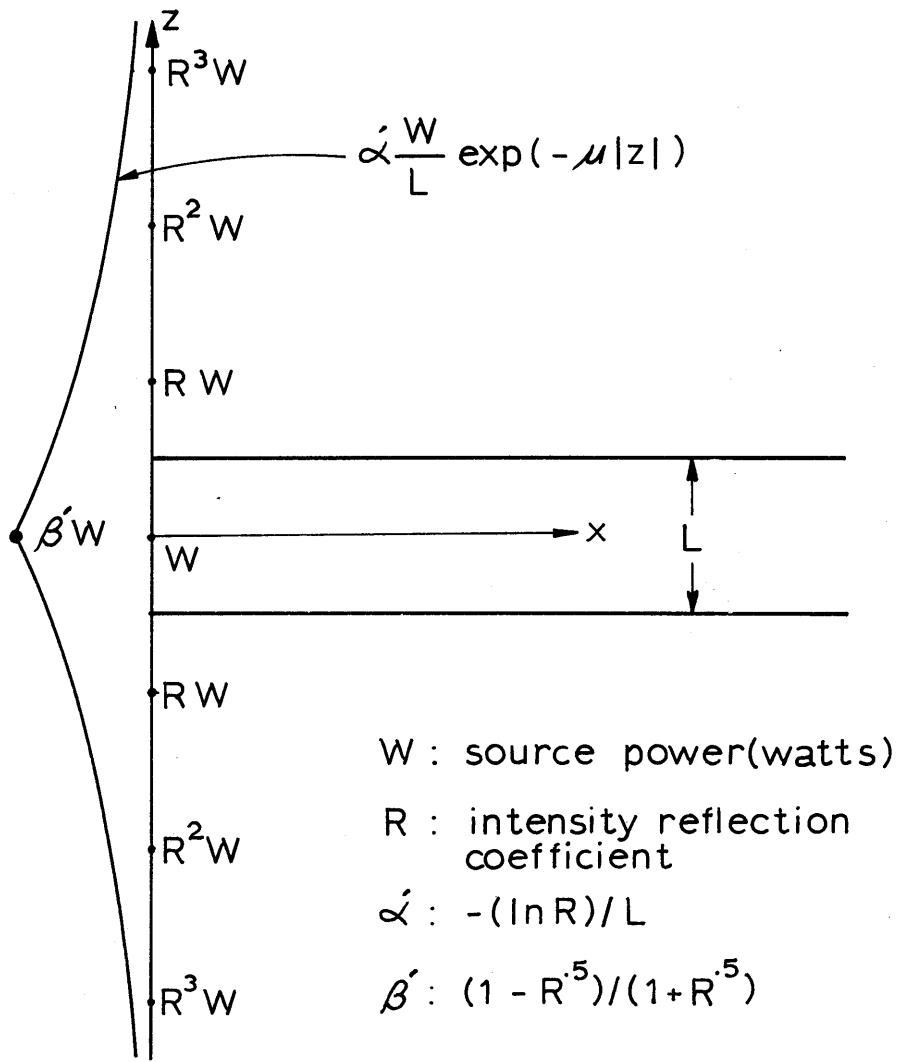
Thus, instead of W, RW, R^2W, ... in each interval, a continuous function of the form

$$W(z) = \alpha' \frac{W}{L} e^{-\mu|z|} \tag{1}$$

was used by Schlatter [1].

In the above equation, μ is given by

$$\mu = -\frac{\ln R}{L} \tag{2}$$

and α', obtained by equating $W(z)$ and the power of the discrete image source in the ith interval ($i \neq 0$), is given by

$$\alpha' = \frac{\sqrt{R} \ln R}{R-1} \tag{3}$$

By equating the sound power in the zeroth interval, which is the original street, an additional factor is added in the form of a point source of strength $\beta'W$,

where

$$\beta' = \frac{1 - \sqrt{R}}{1 + \sqrt{R}} \tag{4}$$

By using the above approximation, the mean square pressure level averaged over the street width L can be expressed as

$$L_p - L_w = 10 \log \left[\frac{\beta'}{x^2} + 2 \int_0^\infty \frac{\alpha' e^{-\mu|z|}}{L^2(x^2 + z^2)} \, dz \right] - 10.83 \qquad (5)$$

where $\quad L_p = 20 \log \dfrac{< P_{rms} >}{P_{ref}}$

$\qquad\qquad L_w = 10 \log \dfrac{W}{W_{ref}}$

$\qquad < P_{rms} > = $ mean square pressure averaged over the street width L

$\qquad P_{ref} = 2 \times 10^{-5} \text{ N/m}^2$

$\qquad W_{ref} = 10^{-12}$ watt

From the plotting of equation (5), Schlatter [1] observed a distance δ, for various values of R, beyond which the L_p drops off by 6 dB per doubling of distance from a source. It is given by

$$\delta = \frac{-7}{\ln R} \qquad (6)$$

and the asymptotes will be parallel to R = 0 line and above it by an amount given by

$$\Delta = 10 \log \frac{1 + R}{1 - R} \quad \text{dB} \qquad (7)$$

Figure 6 shows the distance δ and the difference Δ for several values of the intensity reflection coefficient R.

Figure 6 and above equations (6) and (7) can be used to find a single curve for a general situation of the straight
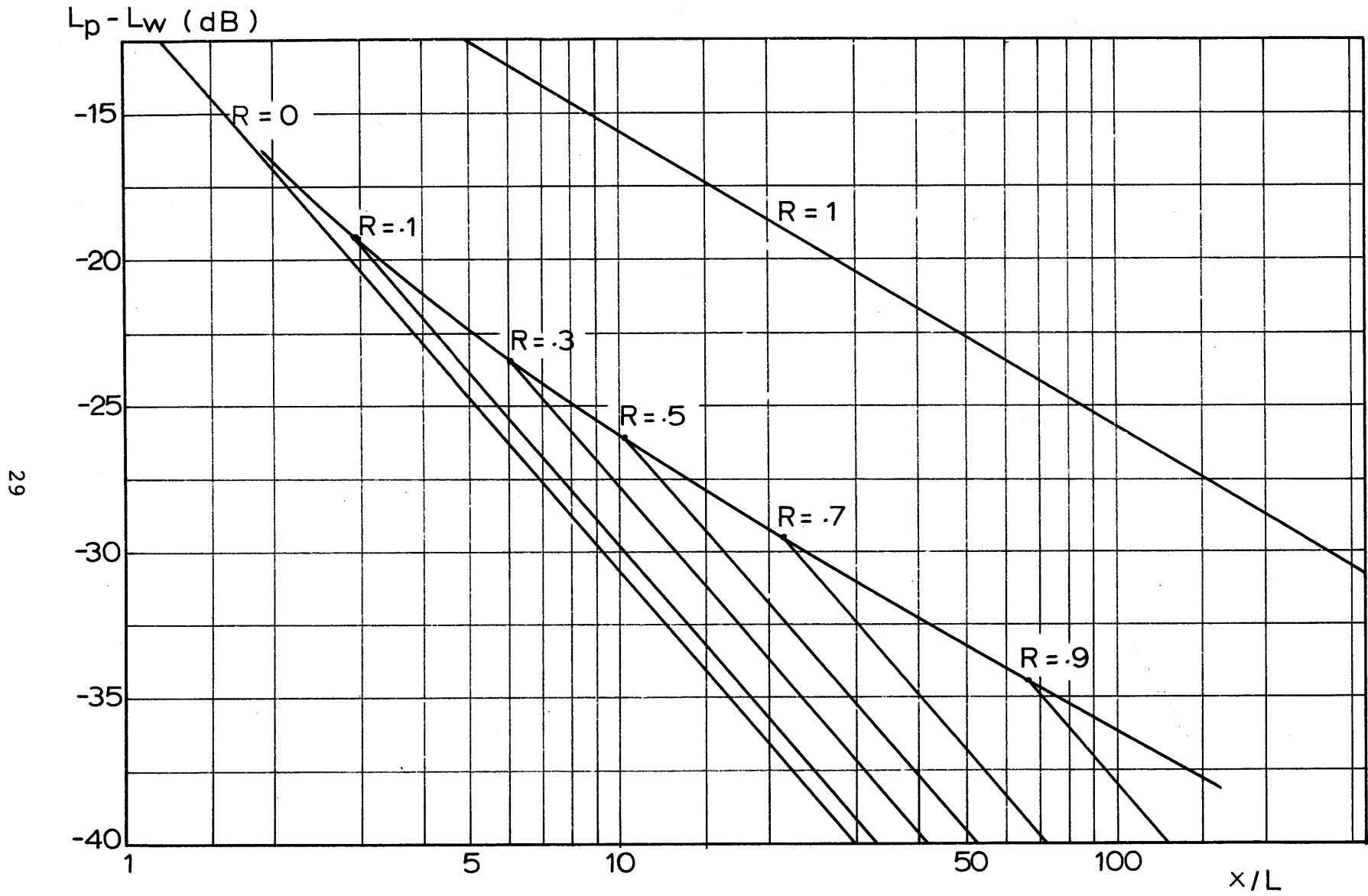
Fig. 6   6 dB d.d. Region

street sound propagation in section C.

B. Intensity Averaging Method (I.A.M.)

Although Schlatter's Method shows how to get an approximate solution to the problem of straight street sound propagation, it cannot be easily used for various situations which arise in physical cases.

In an attempt to collapse the set of curves in Fig. 6 into one single curve, an intensity averaging method is introduced. Using this intensity averaging method, similar attempts will be made in such cases as a straight street with one or more side streets, and also a side street.

1. Straight Street Without Openings

Instead of approximating discrete image sources by a line source, the receiver was changed into a varying strength line receiver as shown in Fig. 7 . Although the above idea is exactly equivalent to changing the sources into a line source, it will be used to make it easier to understand the intensity averaging method.

Consider a sound wave beam of angle $d\theta$ shown in Fig. 7. The intensity at A due to the source of power W is given by

$$I_A = \frac{W}{4\pi} \frac{\exp[(x \tan\theta \ln R)/L]}{r^2} \tag{8}$$

where   r = the distance between the source and receiver

      = x sec θ
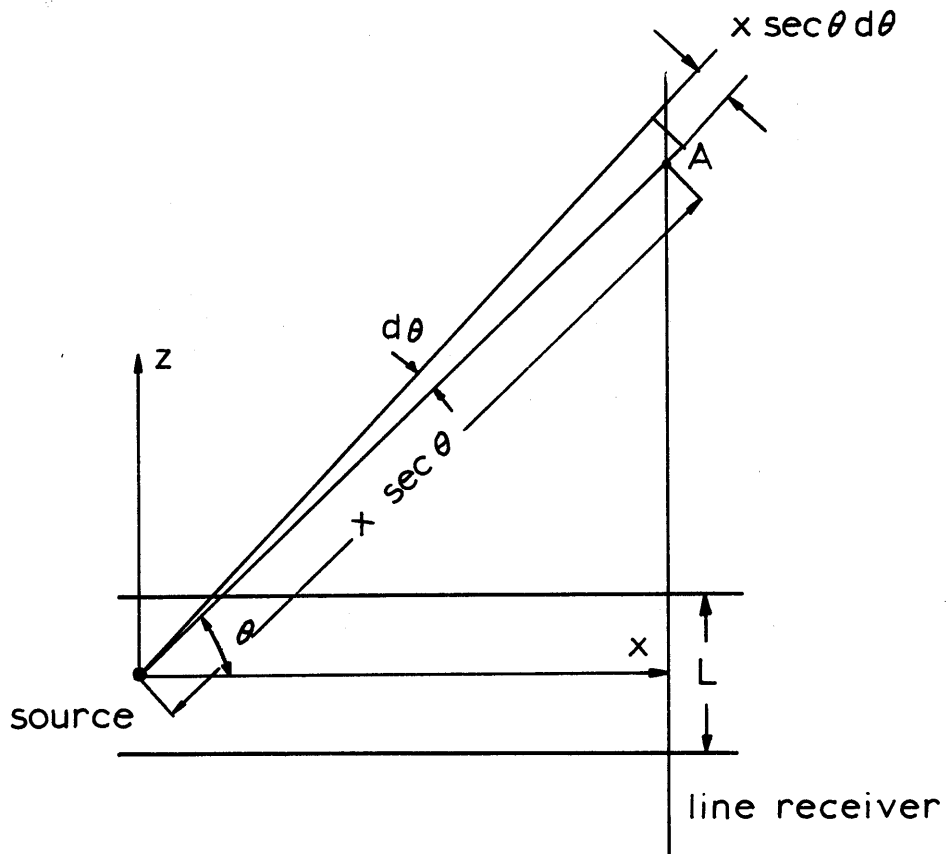
Fig. 7 Model of a Straight Street — I. A. M.

The total power in the beam of angle dθ is given by

$$\Delta W = I_A \cdot \text{arc length within } d\theta \cdot \text{unit height}$$

$$= \frac{W \exp \left(\frac{x}{L} \tan \theta \ln R \right)}{4\pi \, x \sec \theta} \, d\theta \qquad (9)$$

Since all the power goes through the street of width L, the average intensity over the street width, in the direction θ, is given by

$$< I_\theta > = \frac{\Delta W}{L \cos \theta} \qquad (10)$$

where L cos θ is the street width seen from the θ direction.

The mean square pressure averaged over the street width, $< P^2_{rms} >$ is the averaged intensity $< I_\theta >$ integrated in the interval $-\pi/2 < \theta < \pi/2$ and multiplied by the characteristic impedance c. Thus,

$$< P^2_{rms} > = \rho c \int_{-\pi/2}^{\pi/2} < I_\theta > d\theta$$

$$= \frac{\rho c \ W}{2\pi \ x \ L} \int_0^\infty \frac{e^{-\mu x t}}{1 + t^2} \ dt \qquad (11)$$

By rearranging, equation (11) becomes

$$L_p - L_w + 10 \log \frac{L}{\mu} = 10 \log [\frac{2}{\mu x} \int_0^\infty \frac{e^{-\mu x t}}{1 + t^2} dt] - 10.83 \qquad (12)$$

Since the right hand side of equation (12) is a function of μx only, log μx is chosen as the x-axis, and $L_p - L_w + 10 \log \frac{L}{\mu}$ as y-axis. The equation (12) is plotted in Fig. 8 using above axis.
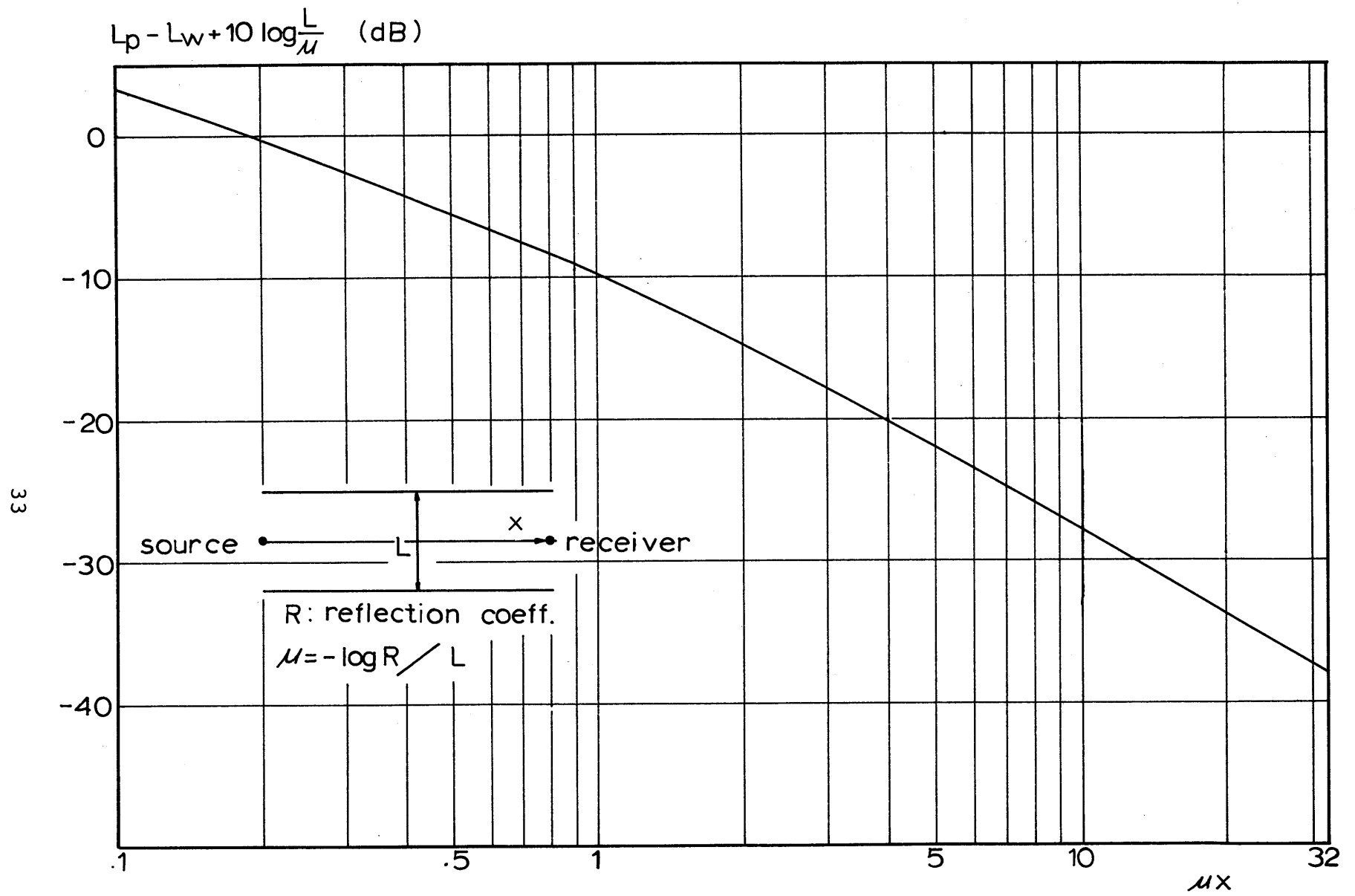
Fig. 8 Lp in Straight Street - I. A. M.

33

2. Straight Street With One Side Street

The same idea that was used in the previous section will be used here with a slight modification.
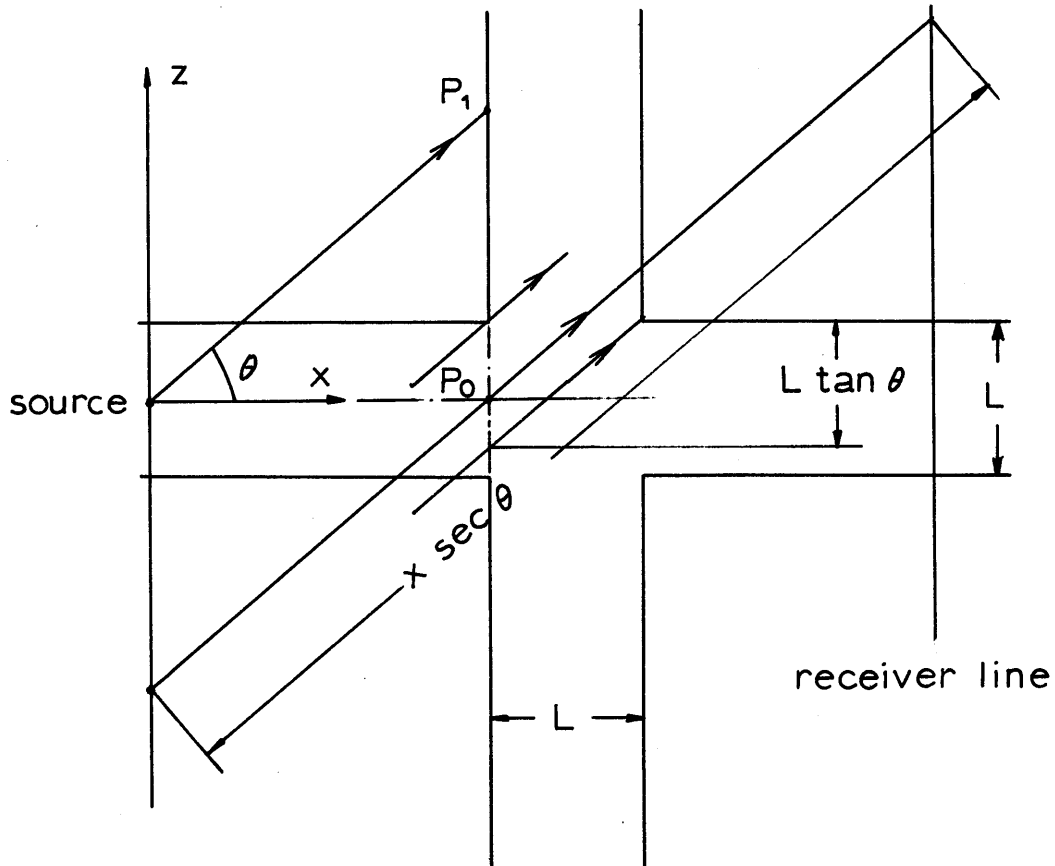
Fig. 9   Model with One Side street – I.A.M.

Since all the waves which get to the receiver must go through the slit ss', the wave beam which passes the point p, is evenly spread over the slit ss'. The idea is that only a portion of the power which goes through the slit ss' gets to the receiver. From geometrical considerations, the net power

that gets to the receiver is the total power which passes the slit ss', multiplied by 1 - tan θ. Thus, the average intensity over the street width at the receiver point, in the direction θ, is given by

$$< I_\theta >_{receiver} \; = \; < I_\theta > \; (1 - \tan \theta)$$

$$= \; \frac{W}{4\pi} \; \frac{1}{xL} \; \exp \, (-\mu x \tan \theta)(1 - \tan \theta)$$

$$(13)$$

The mean square pressure $< P^2_{rms} >$ is twice the intensity summed over θ from 0 to $\pi/4$, and multiplied by the characteristic impedance ρc.

$$< P^2_{rms} > \; = \; 2 \, \rho c \, \frac{W}{4\pi \, xL} \int_0^{\pi/4} \exp(-\mu x \tan \theta)(1 - \tan \theta)d\theta$$

$$(14)$$

By rearranging

$$L_p - L_w + 10 \, \log \frac{L}{\mu} \; = \; 10 \, \log \, [\frac{2}{\mu \, x} \int_0^{\pi/4} \frac{\exp(-\mu x t)(1-t)}{1 + t^2} \, dt]$$

$$- \; 10.83 \qquad\qquad\qquad (15)$$

The equation (15) is plotted in Fig. 10.

$L_p - L_w + 10 \log \dfrac{L}{\mu}$ (dB)

LEGEND

— ·· — no side street
——— 1 side street

μx
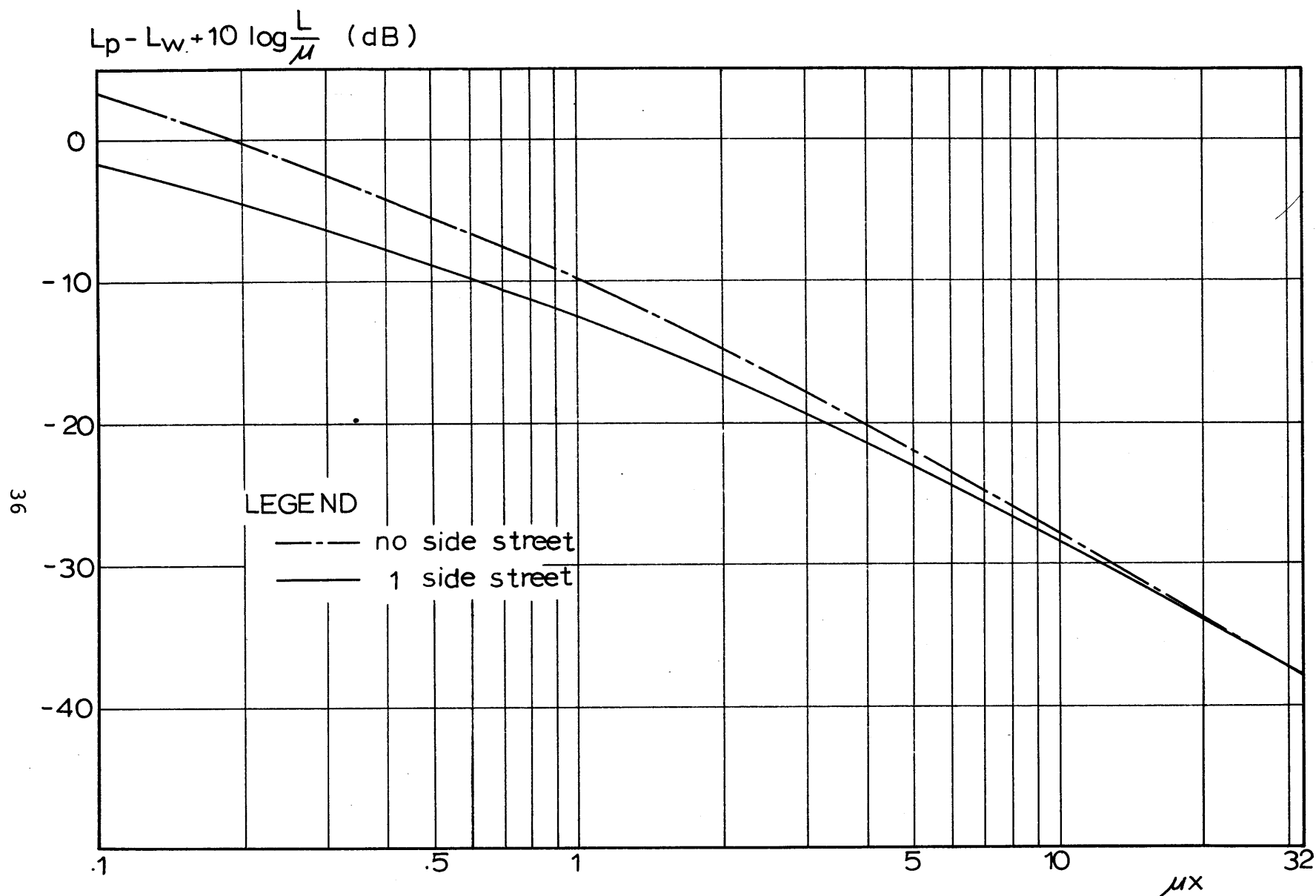
Fig. 10 L_p in Straight Street with One Side Street - I. A. M.

3. Side Street

Just as the previous section, the net power that reaches the receiver must go through the slit ss'. Again, only a portion of the power which passes the slit ss' gets to the receiver.
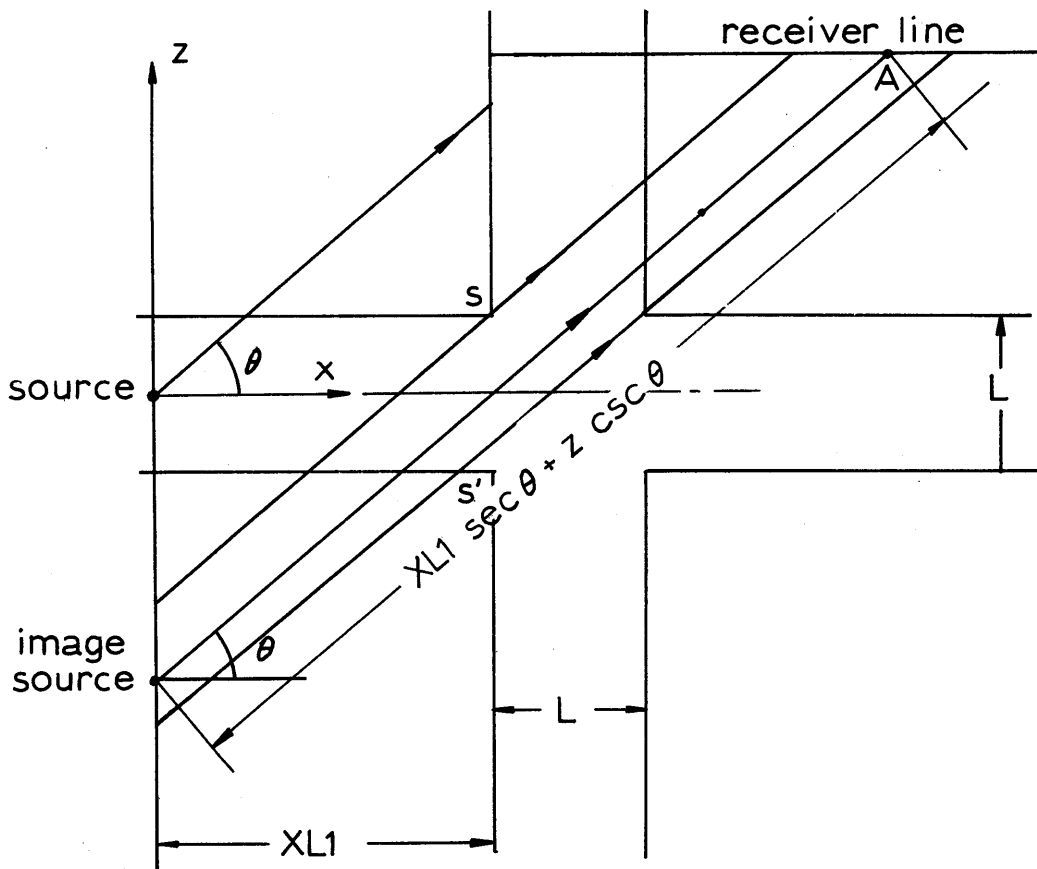
Fig. 11 Model of Side Street — I. A. M.

The intensity at the point A due to a source of power w is given by

$$I_A = \frac{W}{4\pi} \frac{\exp[-\mu(XL1 \tan\theta + z \cot\theta)]}{r^2} \tag{16}$$

37

where   r = source to receiver distance

       = XL1 sec θ + z cosec θ

The total power in the beam of angle dθ in the θ direction is
given by

$$\Delta W \ = \ I_A \cdot \text{arc length within } d\theta \cdot \text{ unit height}$$

$$= \ \frac{W}{4\pi} \ \frac{\exp\ [-\mu(XL1 \tan \theta + z \cot \theta)]\ d\theta}{r} \tag{17}$$

Now, the cases of $0 < \theta < \pi/4$, and $\pi/4 < 0 < \pi/2$
should be considered separately. The case of $0 < \theta < \pi/4$ is
shown in Fig. 12.
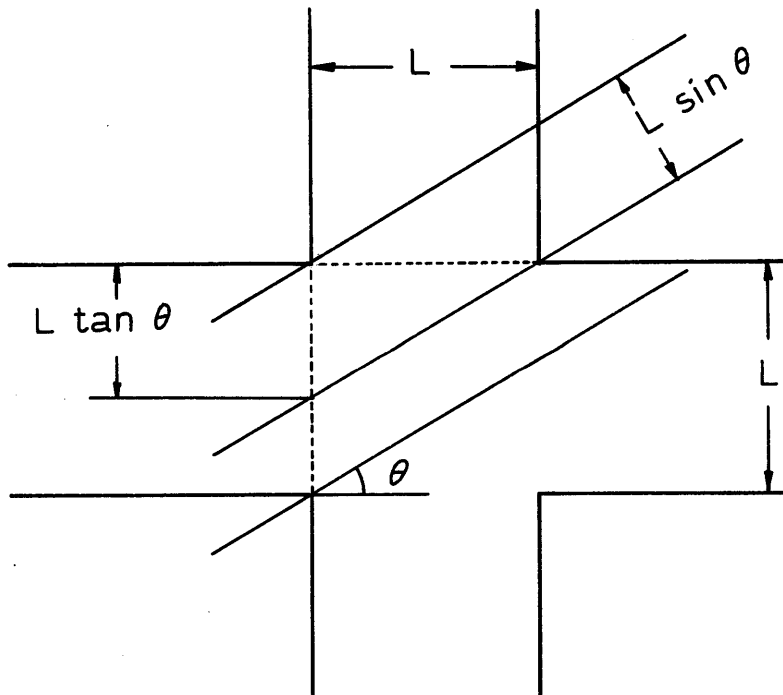
Fig. 12 Model of Side Street When $0 < \theta < \pi/4$

From geometrical considerations, the net power that reaches the receiver is given by

$$\Delta W_{side} = \Delta W \tan \theta \qquad (18)$$

where ΔW is given by the equation (17). Since all the power goes through the side street of width L, the average intensity over the street width, in the θ direction, within the interval $0 < \theta < \pi/4$, is given by

$$< I_\theta >_1 = \frac{\Delta W_{side}}{L \sin\theta} \qquad (19)$$

where $L \sin \theta$ is the width of the side street seen from the θ direction.

The mean square pressure averaged over the street width is the intensity summed over θ from 0 to $\pi/4$ and multiplied by the characteristic impedance ρc. Thus,

$$< P^2_{rms} >_1 = \rho c \int_0^{\pi/4} < I_\theta >_1 \, d\theta$$

$$= \frac{W}{4\pi \, L \, XL1} \int_0^{\pi/4} \frac{\exp \left[-\mu \, XL1 \, (t + \xi/t)\right]}{(1 + \xi/t)(1 + t^2) \, t} \, dt \qquad (20)$$

The case of $\pi/4 < \theta < \pi/2$ is shown in Fig. 13.
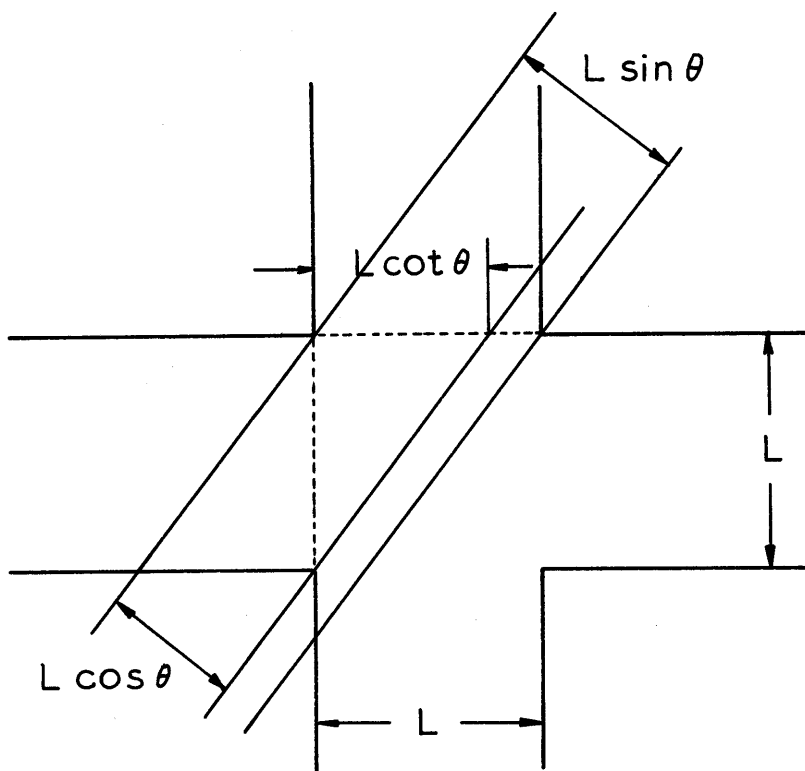
Fig. 13 Model of Side Street When $\pi/4 < \theta < \pi/2$

Here, the total power ΔW given by the equation (17) reaches the side street without being shaded. The average intensity over the street width, in the   direction, within the interval $\frac{\pi}{4} < \theta < \frac{\pi}{2}$, is given by

$$< I_\theta >_2 = \frac{\Delta W}{L \sin \theta} \tag{21}$$

The mean square pressure averaged over the street width is the intensity summed over θ from $\frac{\pi}{4}$ to $\frac{\pi}{2}$ and multiplied by the characteristic impedance ρc. Thus,

$$< P_{rms}^2 >_2 = \rho c \int_{\pi/4}^{\pi/2} < I_\theta > d\theta$$

$$= \frac{W}{4\pi \ L \ XL1} \int_0^1 \frac{\exp[-\mu \ XL1 \ (\frac{1}{t} + \xi t)] \, dt}{(1 + \xi t)(1 + t^2) \ t} \tag{22}$$

40
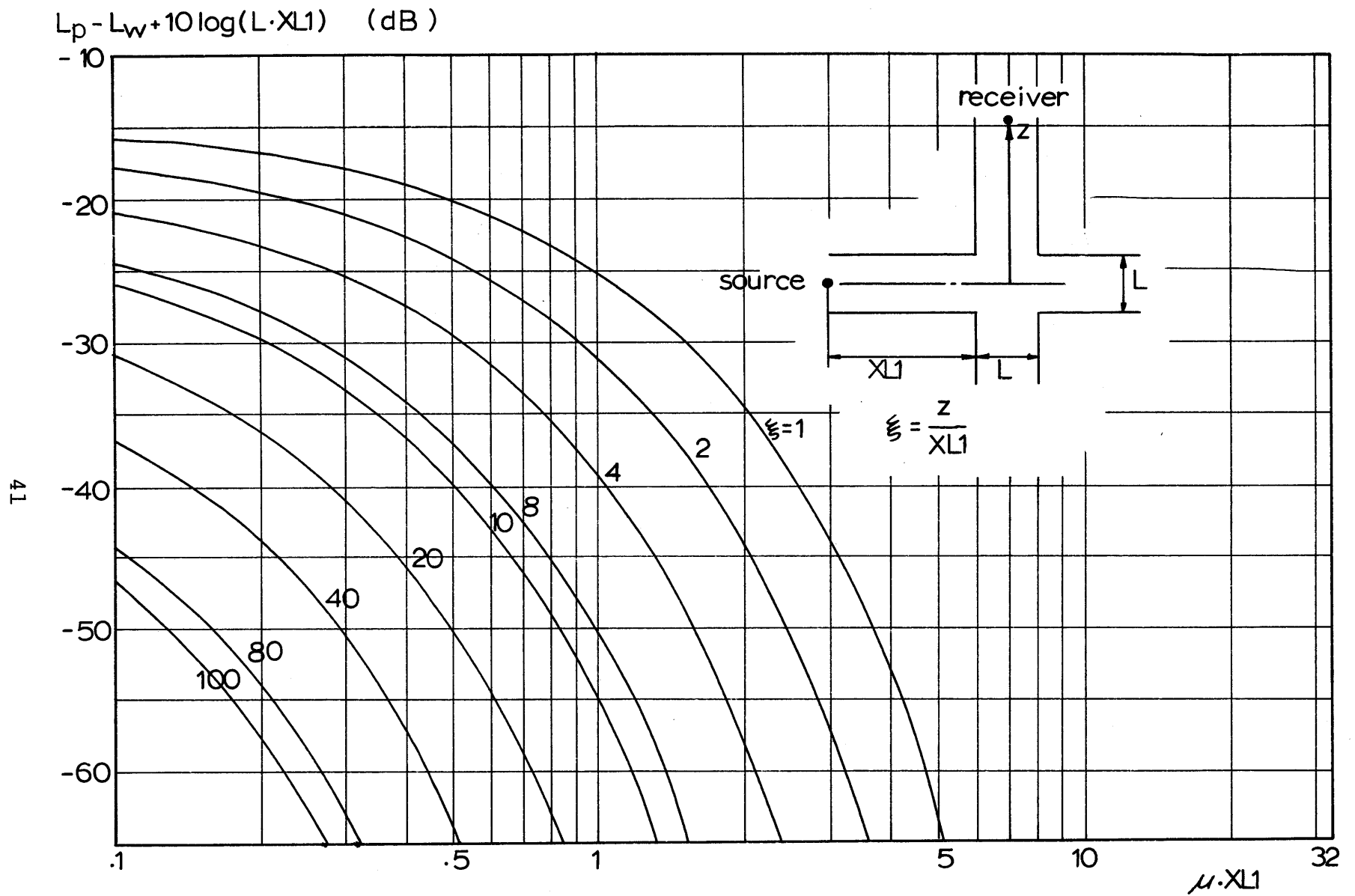
Fig. 14 L_p in Side Street – I. A. M.

$L_p - L_w + 10 \log(L \cdot XL1)$ (dB)

$\xi = 1$

$\xi = \dfrac{z}{XL1}$

$\mu \cdot XL1$

41

$$< P^2_{rms} > = < P^2_{rms} >_1 + < P^2_{rms} >_2 \qquad (23)$$

Substituting $< P^2_{rms} >_1$ and $< P^2_{rms} >_2$, and rearranging,

$$L_p - L_w + 10 \log (L \; XL1) = 10 \log \int_0^1 \frac{\exp[-\mu \; XL1(t+\xi/t)]}{(1+\xi/t) \; (1+t^2)} \, dt$$

$$+ \int_0^1 \frac{\exp[-\mu \; XL1 \; (\frac{1}{t} + \xi t)]}{(1+\xi t) \; (1+t^2) \; t} \, dt \qquad - 10.83 \qquad (24)$$

The equation (24) is plotted in Fig. 14 .

C. Computer Solution - Discrete Image Sources (D.I.S.)

Since calculating the sound pressure due to each image source at a various receiver points is a tedious and cumbersome job, attempts have been made to get an approximate solution to the problem. From the result of Schlatter's [1] method and intensity averaging, it is now possible to get nondimensional parameters which will enable us to arrange a bulk of data produced by computer solutions in several cases shown in Fig. 2 into a simple nomogram or a design chart.

1. Straight Street With no Side Streets

This is the simplest case of all, and the same algorithm can be used for each image sources only by changing the distance between source and receiver.
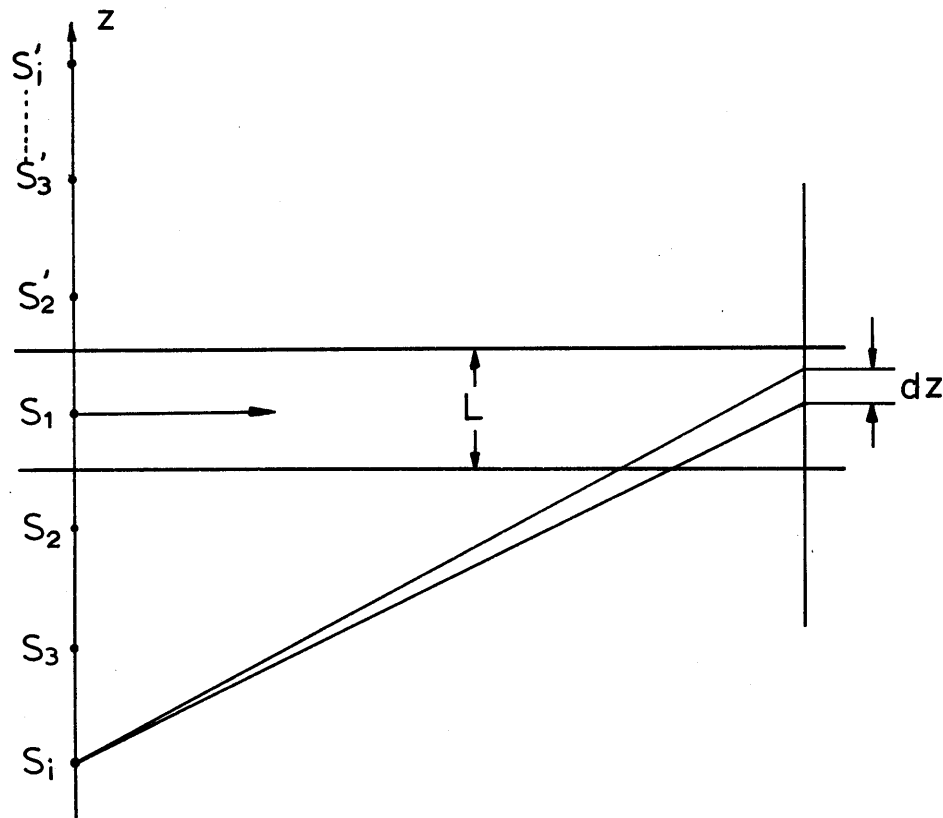
Fig. 15 Model of Straight Street — D. I. S.

For illustration, choose an image source S_i. The distance between source and receiver is given by

$$r = [x^2 + \{(i - 1)L + z\}]^{1/2}.$$

Intensity at the receiver can be written as

$$I_z = \frac{W}{4\pi} \frac{\exp\left[(i-1)\ln R\right]}{r^2} \qquad (25)$$

The total power that passes through dz is given by

$$\Delta W = \frac{W}{4\pi} \frac{\exp\left[(i-1)\ln R\right]}{r^2} dz \qquad (26)$$

The mean square pressure averaged over the street width L, due to S_i, is given by

$$<P_{rms}^2> = \rho c \frac{W}{4\pi L} \int_{-L/2}^{L/2} \frac{\exp\left[(i-1)\ln R\right] dz}{x^2 + \left[(i-1)L + z\right]^2} \qquad (27)$$

Therefore, the total mean square pressure level averaged over street width L, due to all the source S_1, S_2, S_2', S_3, S_3', ..., is given by

$$<P_{rms}^2> = \rho c \frac{W}{4\pi L} \int_{-L/2}^{L/2} \frac{dz}{x^2 + z^2}$$

$$+ 2 \rho c \frac{W}{4\pi L} \sum_{i=1}^{imax} \int_{-L/2}^{L/2} \frac{\exp\left[(i-1)\ln R\right] dz}{x^2 + \left[(i-1)L + z\right]^2} \qquad (28)$$

The first term in (28) corresponds to the i = 1 case and the factor 2 in the second term comes from the symmetry of the source distribution. The upper limit of summation 'imax'
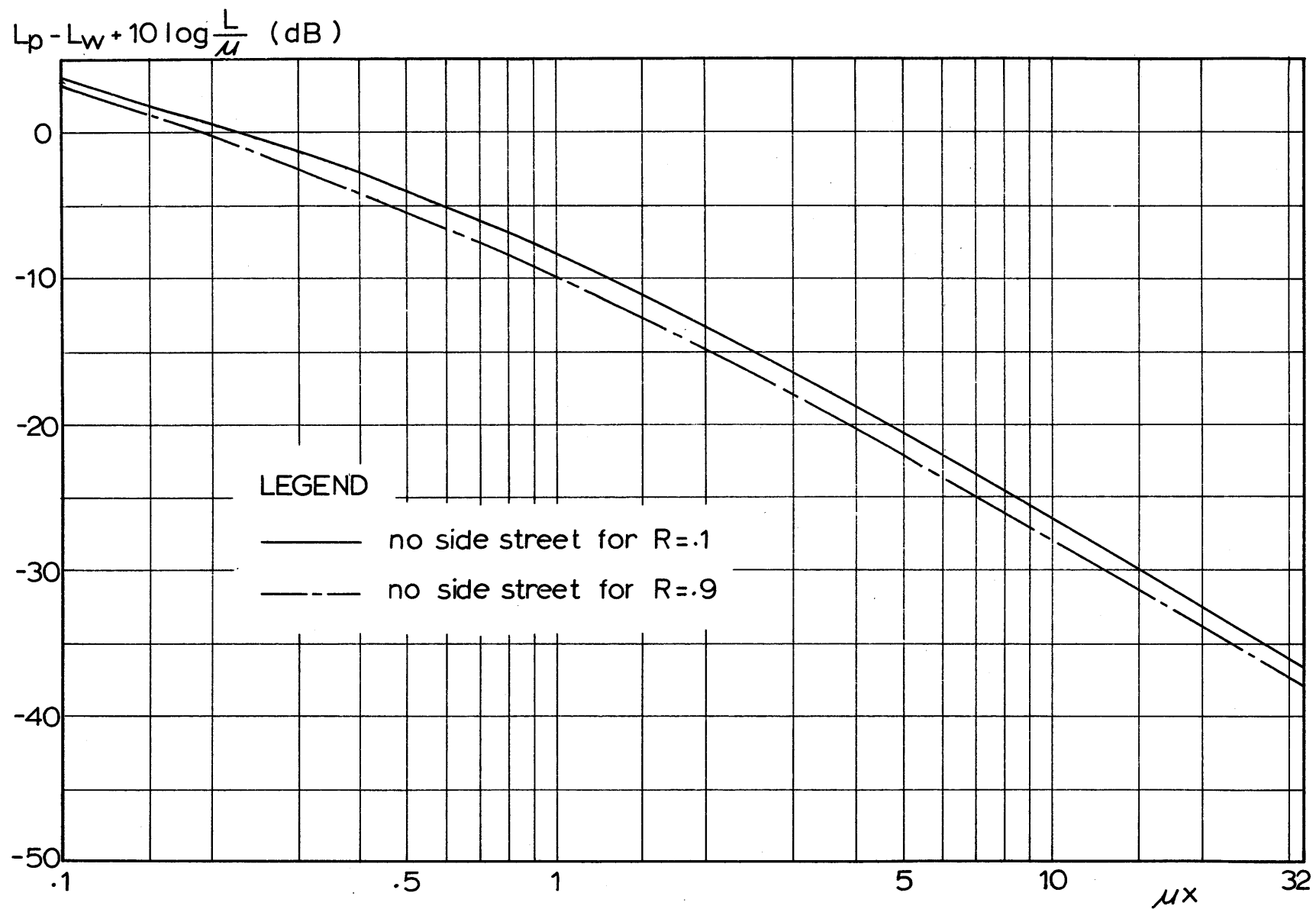
Fig. 16 L_p in Street Street - D.I.S.

The y-axis is labeled $L_p - L_W + 10 \log \frac{L}{\mu}$ (dB) with values from 0 at top down through -10, -20, -30, -40, -50.

The x-axis is labeled μx with values .1, .5, 1, 5, 10, 32.

LEGEND

——— no side street for R=.1

—·—·— no side street for R=.9

45

was decided such that when the sum of the pressures due to the sources from i + 1 to i + 10 is less than 1% of the sum up to i^{th} sources. The result of computation of equation (28) is shown in Fig. 16 using $L_p - L_w + 10 \log \frac{L}{\mu}$ and $\log \mu x$ as x- and y-axis, which were obtained by intensity averaging method in Section B.

As shown in Fig. 16 , the difference in sound pressure level, ΔL_p, between the cases of various values of the intensity reflection coefficient R, is almost constant with respect to x except when x is of order of 10^{-1}. The difference ΔL_p will be estimated by making use of equations (7), (12) and Fig. 6 and Fig. 16 . After that, the set of curves in Fig. 16 will collapse into a single curve.
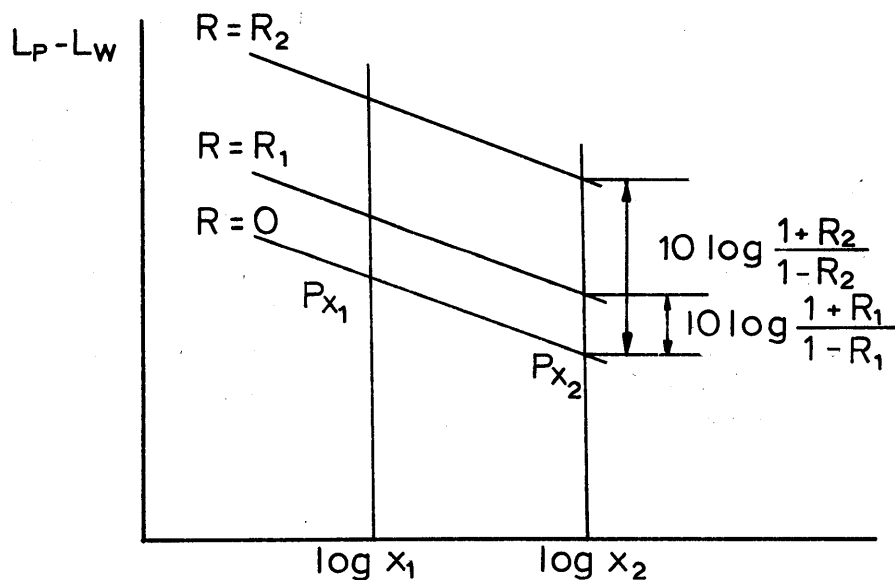
Fig.17 Estimation of Δ

46

By assuming that above lines are inside the 6 dB per doubling of distance region in Fig. 6,

$$P_{x_1} - P_{x_2} = 20 \log \frac{x_2}{x_1} \tag{29}$$

for a given value of R. The points x_1 and x_2 are chosen such that

$$\mu_1 x_1 = \mu_2 x_2 \tag{30}$$

where $\quad \mu_1 = - \dfrac{\ln R_1}{L}, \quad \mu_2 = - \dfrac{\ln R_2}{L}.$

By observing the pressure level difference $\Delta = 10 \log \dfrac{1+R}{1-R}$ in Fig. 17, and the changes in x, y coordinates from Fig. 17 to Fig. 16 , the difference ΔL_p in Fig. 16 is given by

$$\Delta L_p = 10 \log \left(\frac{\mu_1}{\mu_2} \cdot \frac{1+R_1}{1-R_1} \cdot \frac{1-R_2}{1+R_2} \right) \tag{31}$$

Using $L_p - L_w + 10 \log \alpha$ as a new y-axis, which is equivalent to $10 \log \left(\dfrac{<P_{rms}^2>}{\mu \, \rho c} \dfrac{4\pi L}{W} \right) + \Delta L_p - 10.83$, where α is given by, setting $R_1 = 0.1$,

$$\alpha = \frac{2.81 \, (1-R)}{\mu^2 \, (1+R)} \tag{32}$$

A curve which represents a wide range of cases of street propagation is obtained (Fig. 18).

47
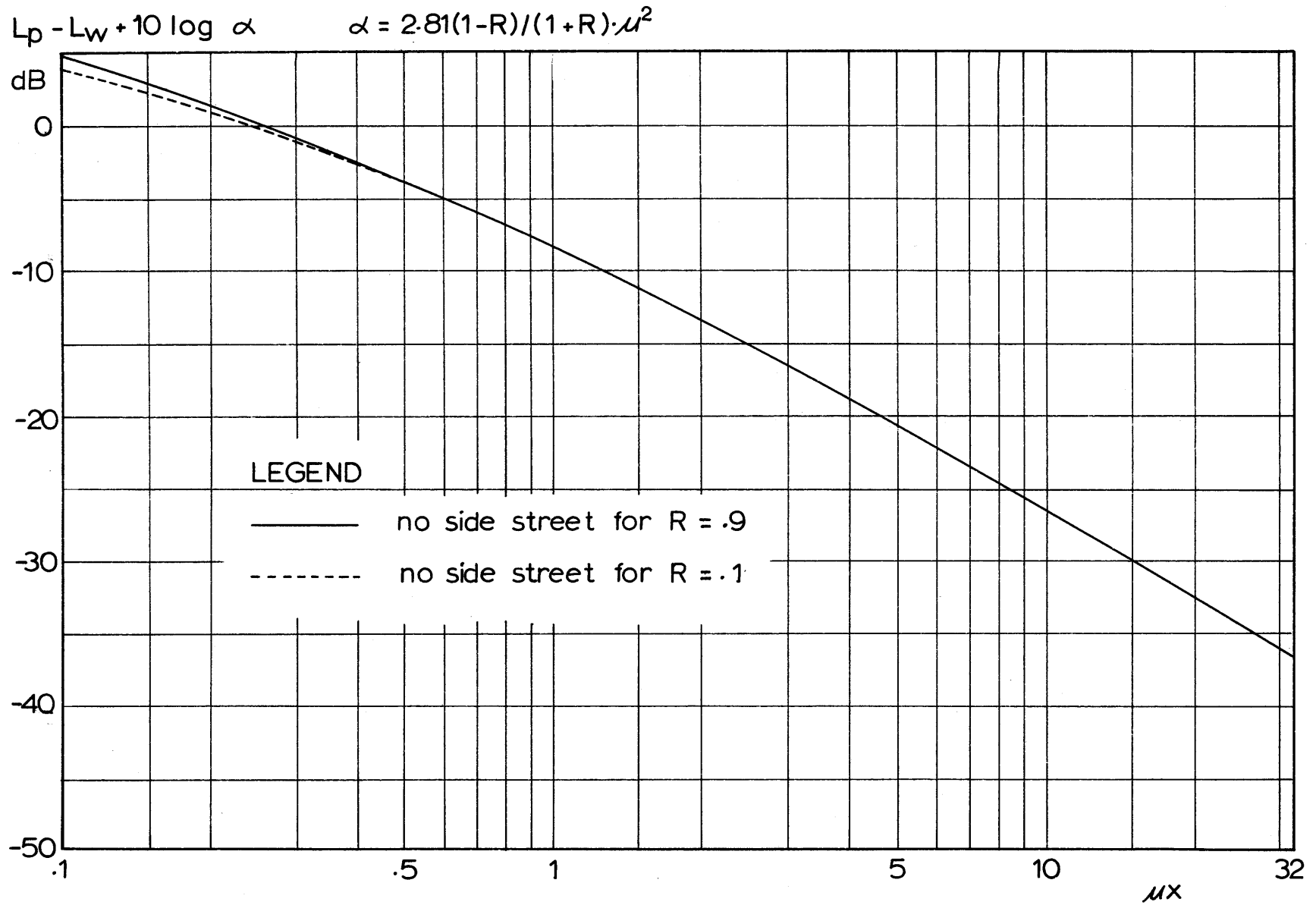
Fig. 18 Single Curve for Straight Street

2. Straight Street With One Side Street

The sound pressure contribution due to S_i in Fig. 19 is given by

$$\frac{<P_{rms}^2>}{\rho c} \frac{4\pi}{W} = \frac{1}{L} \int_{z_1}^{z_2} \frac{\exp\{[(i-1)+INT(.5+\frac{|z|}{L})] \ln R\} \, dz}{x^2 + [(i-1)L+z]^2} \quad (33)$$

where INT(F) means the largest integer $\leq$ F, and z_1 and z_2 are the intersecting points of the receiver line with lines S_iA and S_iB, respectively.
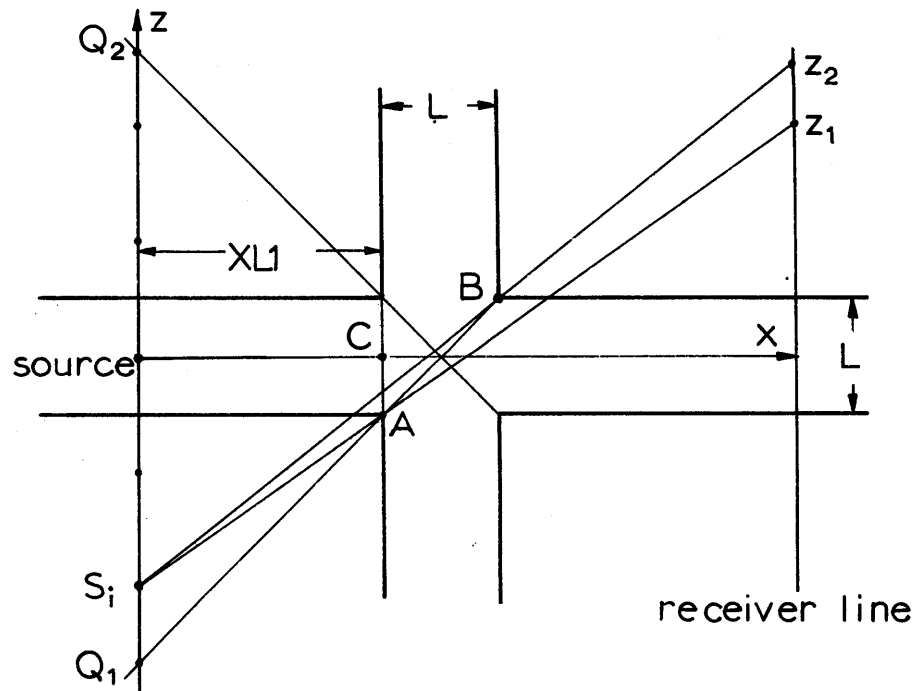
Fig. 19 Model with One Side Street − D. I. S.

The number of sources which contributes to the sound pressure at the receiver position is $2 \cdot imax - 1$, where $imax$ is the largest i between Q_1 and Q_2. Therefore, the total mean square pressure averaged over the street width L is given by

$$\frac{< P^2_{rms} >}{\rho c} \frac{4\pi}{W} = \frac{1}{L} \int_{z_1}^{z_2} \frac{\exp\left[INT(.5 + \frac{|z|}{L}) \ln R \right] dz}{x^2 + z^2}$$

$$+ \frac{2}{L} \sum_{i=2}^{imax} \int_{z_1}^{z_2} \frac{\exp\left\{ [(i-1) + INT(.5 + \frac{|z|}{L})] \ln R \right\} dz}{x^2 + [z^2(i - 1)L + z]^2}$$

(34)

where
$$imax = INT(1.5 + \frac{XL1}{L})$$

$$z_1 = L(\frac{i - 1.5}{XL1} x - i + 1)$$

$$z_2 = L(\frac{i - .5}{XL1 + L} x - i + 1).$$

The equation (34) was evaluated for various values of R, and for various locations of source and receiver points. The position of the side street was also changed to find out the effect of the location of the side street.

To plot the results, the same coordinate system that was used in Fig. 10 of intensity averaging method, is used,

Fig. 20 Lp in a Straight Street with One Side Street-D. I. S.

The y-axis is labeled: $L_p - L_w + 10 \log \frac{L}{\mu}$ (dB), with values 0, -10, -20, -30, -40, -50.

The x-axis is labeled μx, with values .1, .5, 1, 5, 10, 32.

LEGEND

————————	R = .9, XL1 = 4L
—·—·—·—	R = .9, XL1 = .5L
— — — —	R = .1, XL1 = 4L
- - - - - -	R = .1, XL1 = .5L
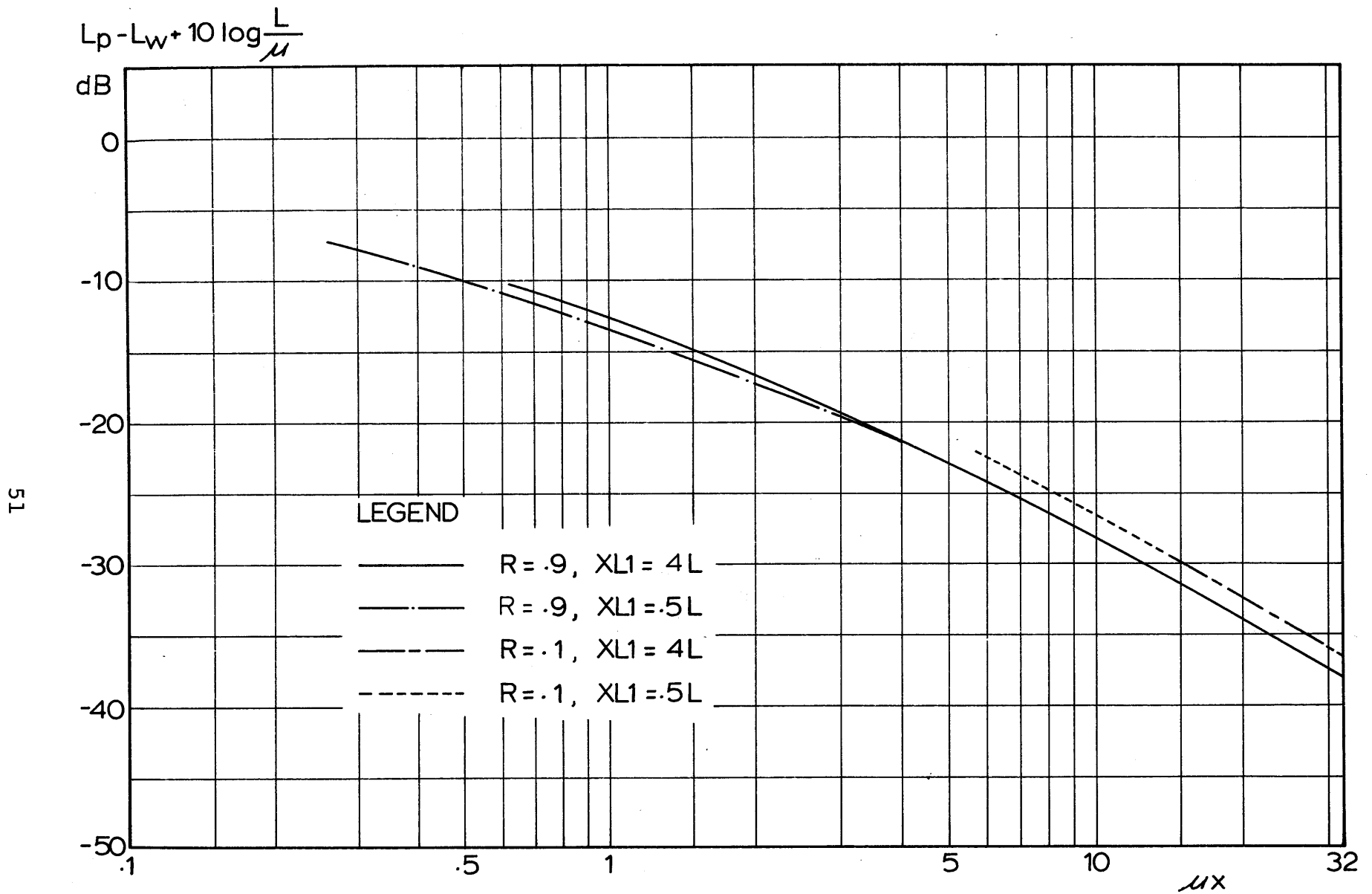
which is shown in Fig. 20. As is obvious from Fig. 20, the position of the side street does not make an appreciable difference, which is to be expected as we are dealing only with the average sound level across the street.

In Fig. 20, a constant pressure level difference between two different values of R is observed just as in Fig. 18. Another observed fact from the computer output is that even in the case when the source is moved to the side street entrance which is shown by the position C in Fig. 19, there was still little difference in the pressure level as long as we keep the source to receiver distance x constant. This fact and above mentioned constant pressure level difference observed give us a hint that the same non-dimensional parameter α could be used to get a single curve for this case just as Fig. 18 for the former case. The only difference between these two cases would be a certain amount of drop in sound level. Using the parameter α, the desired curve for the straight street with one side street is obtained as shown in Fig. 21.

We now have two curves which can explain the cases of receiver points 1, and 2 in Fig. 2 for any value of R. It is now natural to expect that a similar phenomena will happen if we have more than one side streets.

3. Straight Street With More Than One Side Streets

A computer program was developed to estimate the sound pressure level at a receiver point in a straight street with an arbitrary number of side streets. Computations for the case of 2 and 3 side streets are done, and the results are shown in Fig. 21.

As expected, the sound pressure level drops off suddenly by a certain amount whenever receiver passes a side street. The pressure level drop L_p decreases as the number of the side street increases. In the limit, the drop L_p will become zero; at that point, only the waves propagating parallel to the centerline of the street will remain. In other words, the waves does not see the wall of the street at all, just as in open field propagation at a distance sufficiently far from the source. Thus, all the cruves asymptotes to the curve of no side street case.
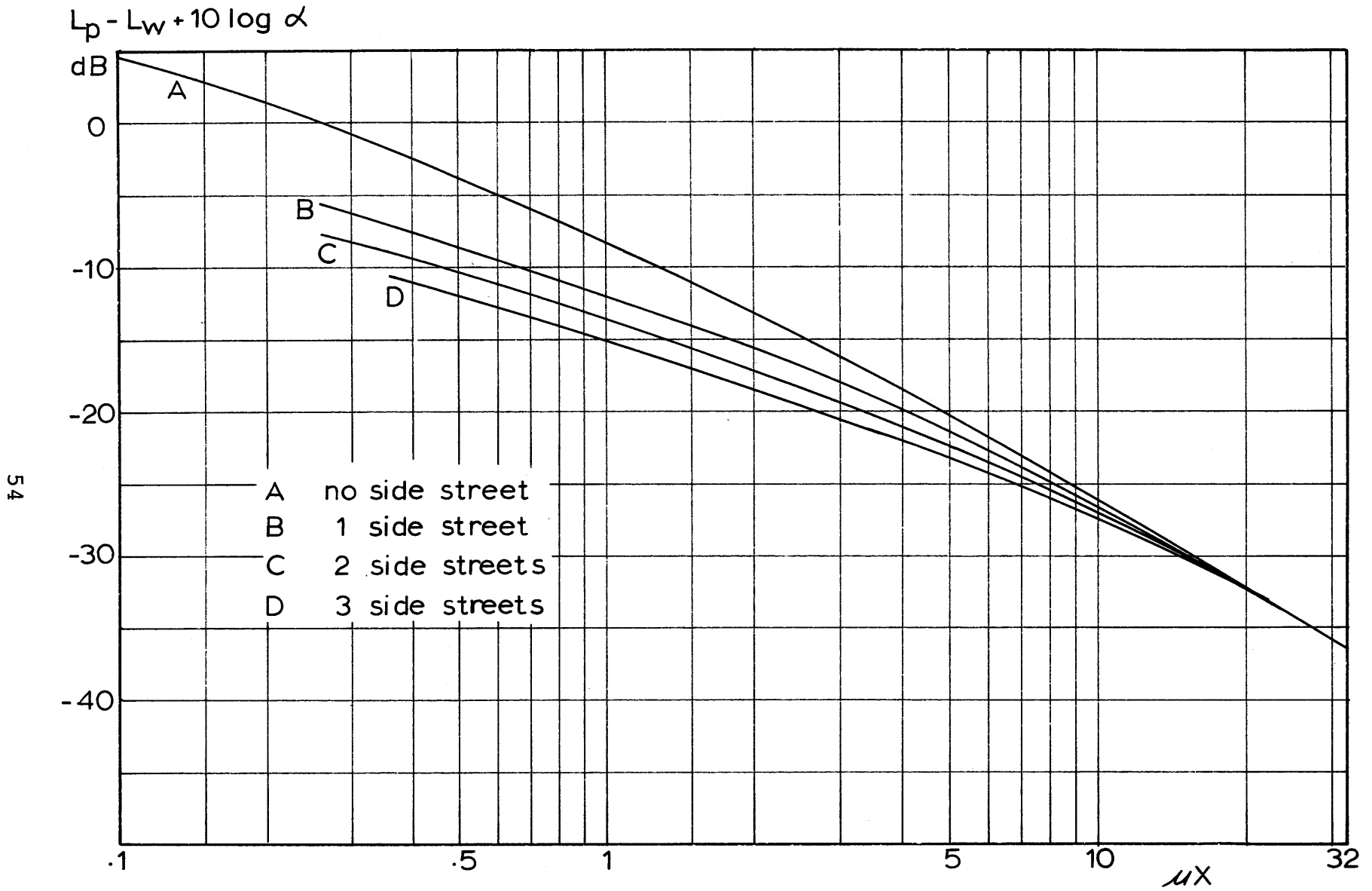
Fig. 21 L_p in a Straight Street with Several Side Streets - D. I. S.

Chart labels and axes:

$L_p - L_w + 10 \log \alpha$

dB

A   no side street
B   1 side street
C   2 side streets
D   3 side streets

μx

4. The First Side Street

Fig. 22 Model of the First Side Street - D. I. S.

The total sound pressure level due to all the sources which can reach the receiver position shown in Fig. 22 is given by

$$L_p - L_w + 10 \log L_2 = 10 \log \sum_{i=1}^{\infty} \int_{x_1}^{x_2} \frac{\exp[((i-1) + INT(\frac{x - XL1}{L_2})) \ln R] \, dx}{x^2 + [(i-1)L_1 + z]^2}$$

$$- \quad 10.83 \qquad\qquad (35)$$

where $\quad x_1 = [\dfrac{z + (i - 1)L_1}{L_1/2 + (i - 1)L_1} + 1]\ XL1$

$$x_2 = [\dfrac{z + (i - 1)L_1}{L_1/2 + (i - 1)L_1} + 1]\ (XL1 + L_2) \quad \text{when } i \le imax$$

$$x_2 = [\dfrac{z + (i - 1)L_1}{-L_1/2 + (i - 1)L_1} + 1]\ XL1 \qquad \text{when } i > imax$$

$$imax = INT(1.5 + \dfrac{XL1}{L_2})$$

The "imax" tells us whether the source is above or under the point Q which is the intersection of the line ABQ and the source line in Fig. 22.

The result is plotted using $L_p - L_w + 10 \log (XL1\ L_2)$ and $\log \mu x$ as y and x-axis, respectively, which were found by intensity averaging Method in the hope of getting a simple set of curves which have been suggested by Fig. 14 . From the plotting of the equation (35), it is observed that the curves are still dependent on the values of R.

To remove the R dependence which is obviously undesirable to obtain a simple design chart or a nomogram, a large number of computatio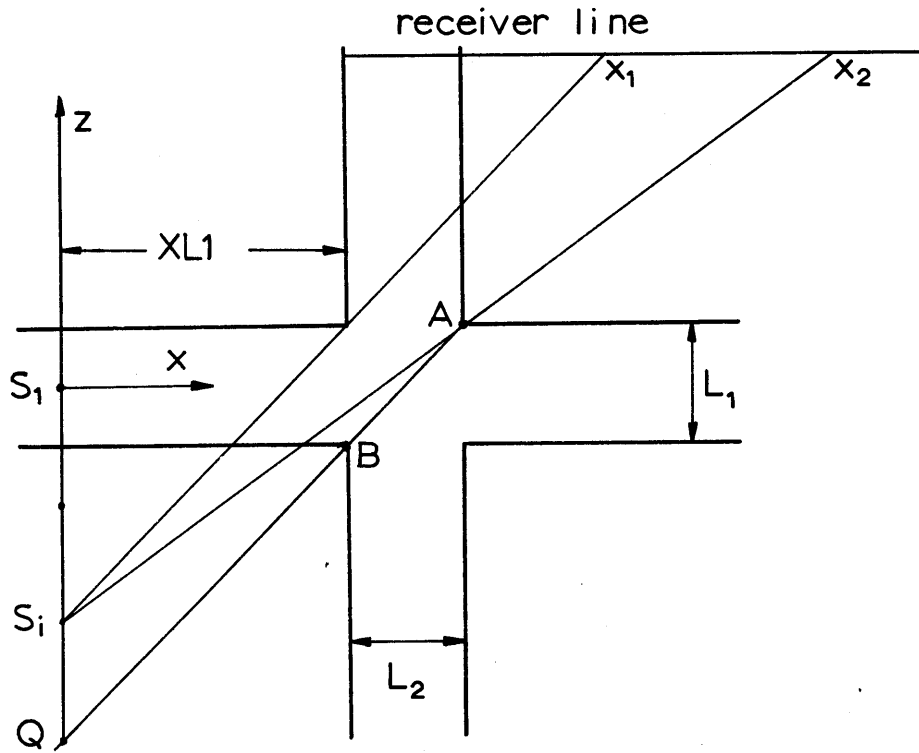ns were carried out for various cases of the side street sound propagation. The results were plotted using $\log \mu x$ and $L_p - L_w + 10 \log (XL1\ L_2)$ as x- and y-axis, respectively, to see if there is any recognizable pattern. From above plot- tings, it was found that, by choosing $L_p - L_w + 10 \log (XL1\ L_2 \ R^{0.8})$ as a new y-axis, we would be able to get a set of curves

which are almost independent of the value of R, which is shown
in Fig. 23 .
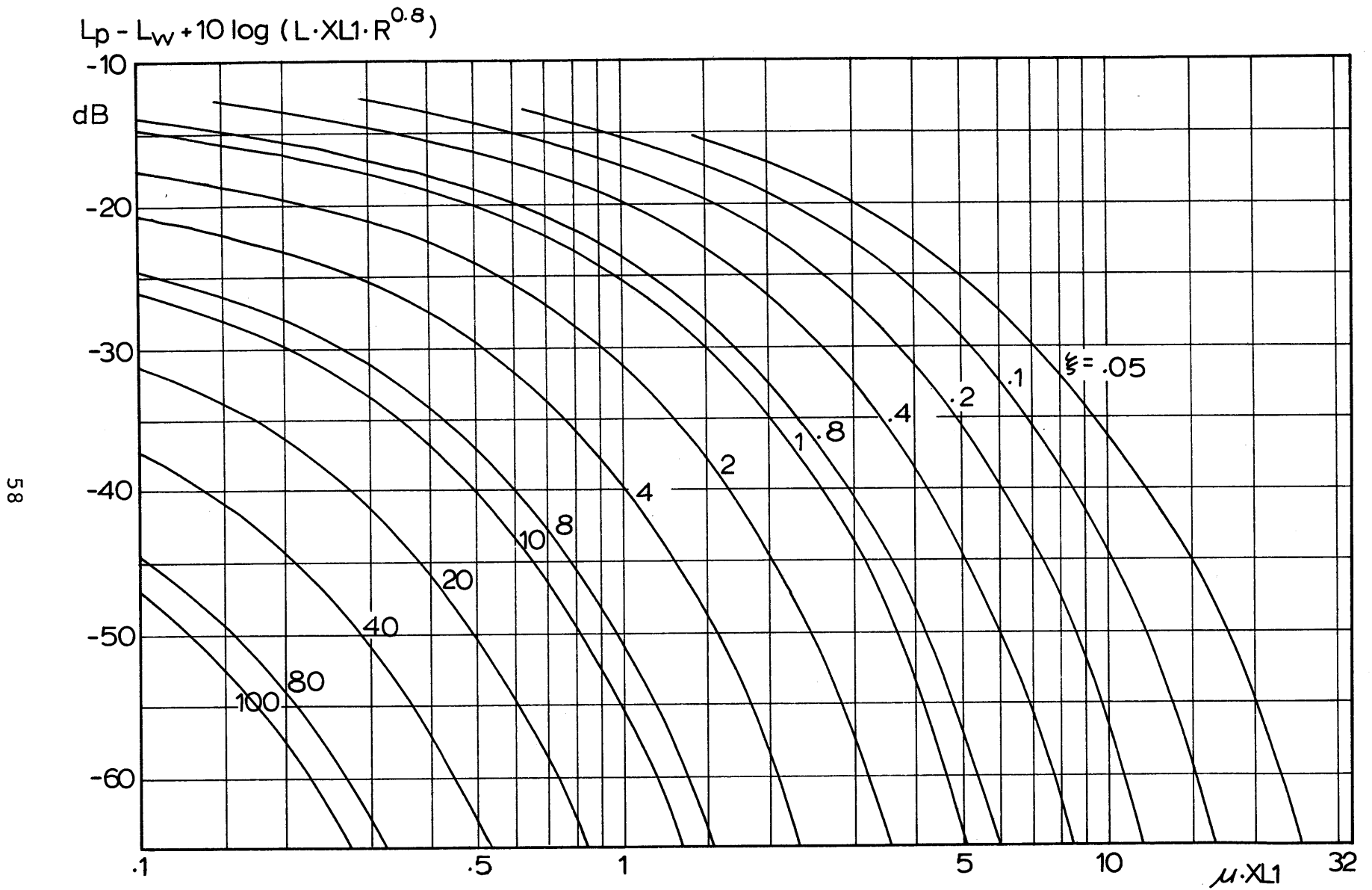
Fig. 23 Lp in the First Side Street-D.I.S.

$L_p - L_w + 10 \log (L \cdot XL1 \cdot R^{0.8})$

$\mu \cdot XL1$

$\xi = .05$

58

5. The Second Side Street

A computer program was developed for the second side street propagation which can be easily modified to be used in N^{th} side street propagation if used in combination with the computer program for the case of a straight street with an arbitrary number of side street.

For illustration, take the case of the source S_3 and the receiver which is located in the Nth side street ($N \geqq 2$), the wave beam should go through the interval AB. Also, it must not be blocked by any of the cross-lines of the side streets until it reaches the receiver line.

Unlike the straight street case, in which the wave travels the distance of the line drawn from an image source to the receiver, in the side street case, the wave travels the distance of the line drawn from an image source to the 'lifted' receiver position. The 'Lift' which accounts for the number of reflections, N_R, in the region between the first side street and the Nth side street,, is expressed as

$$\text{Lift} = N_R \cdot \text{width of the street L} . \tag{36}$$

N_R can be easily obtained by

$$N_R = \text{INT} [(z_0 + L/2)/L], \tag{37}$$

where z_o is the distance from the centerline of the straight street to the intersection of the wave beam and the wall of the Nth side street which is nearer to the source.

From Fig. 24, only those image sources which are located between the points z_1 and z_2 can contribute to the Nth side street ($N \geq 2$). The result of the computation showed no recognizable pattern as in the straight street case or the first side street case.

The case R = 0.9 is computed and shown in Fig. 25. The dotted lines are the curves for the first side street.

D. Discussion

1. Intensity Averaging and Computer Solution

Comparing the results from intensity averaging and Computer Solution, it turned out that the intensity averaging is quite accurate in the straight street propagation either with or without side streets with maximum deviation of 2 dB [Fig. 26].

The intensity averaging method also estimated the sound level in the first side street quite accurately with maximum deviation of 2 dB when R was set to 0.9. [Fig. 27]. The intensity averaging method, even with its failure in certain cases, played a major role to find the simple nomogram.
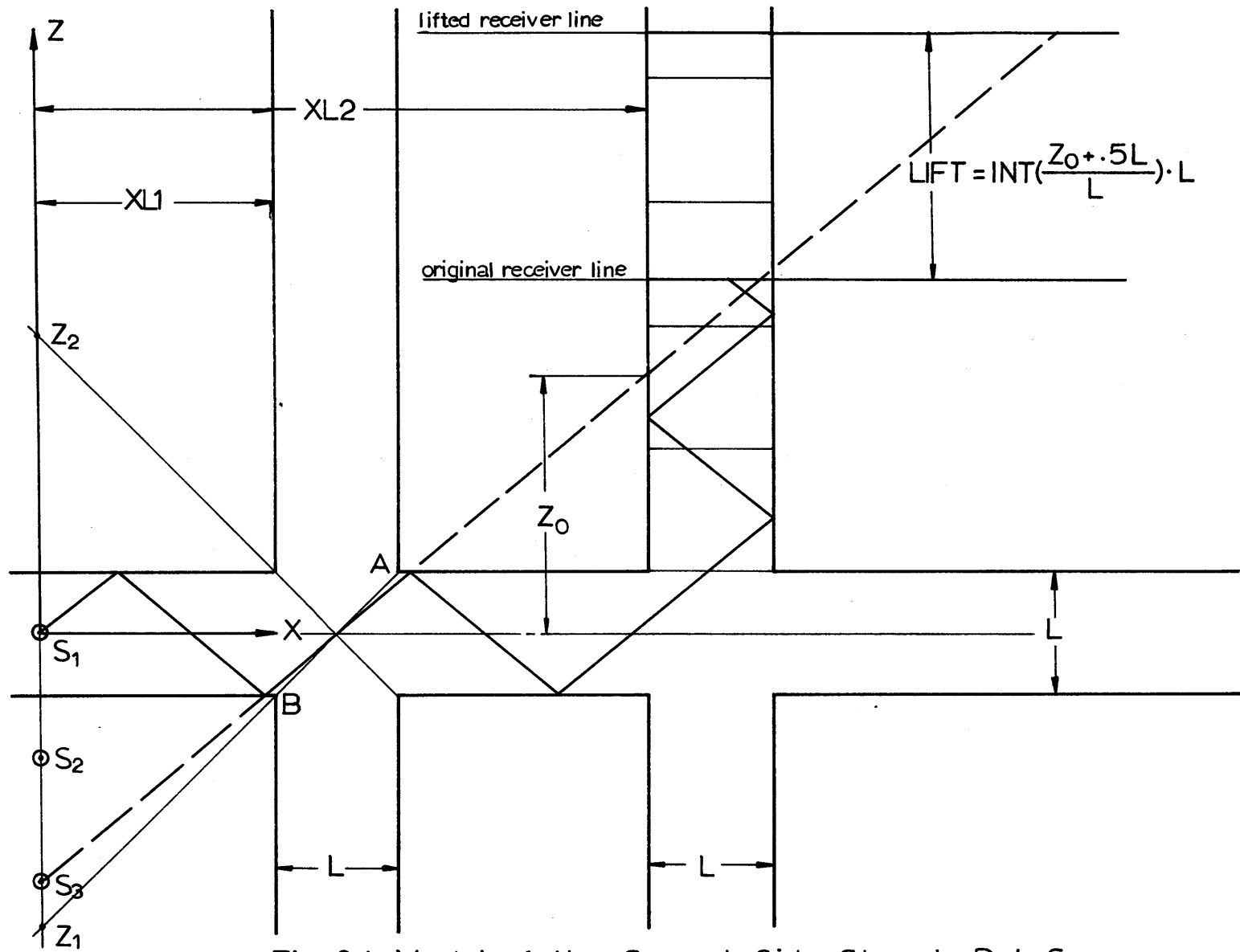
Fig. 24 Model of the Second Side Street-D. I. S.
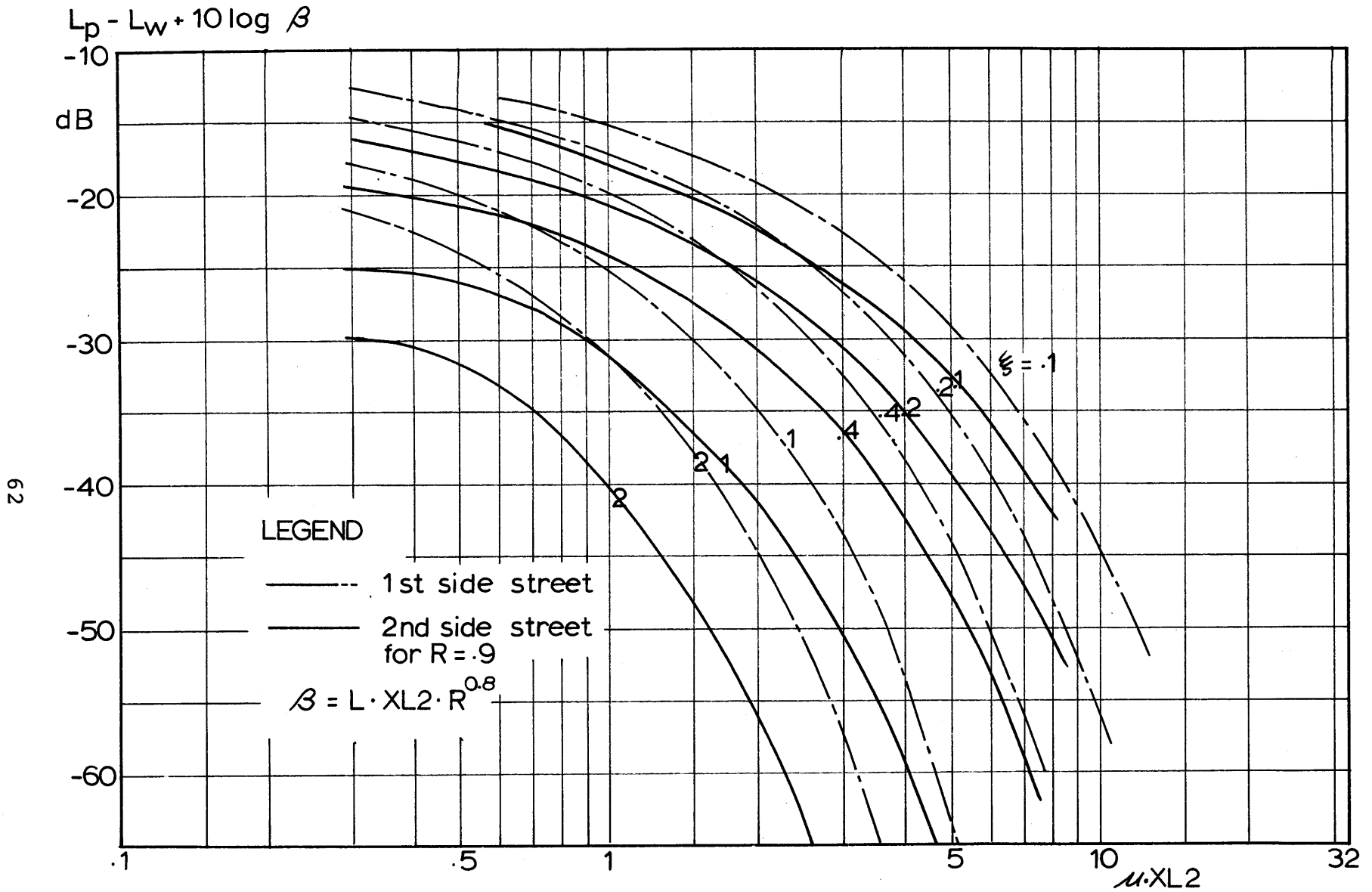
Fig. 25 L_p in the Second Side Street-D.I.S.

The y-axis label: $L_p - L_W + 10 \log \beta$ (dB)

The x-axis label: $\mu \cdot XL2$

LEGEND

- - - - - 1st side street
——— 2nd side street
for R = .9

$\beta = L \cdot XL2 \cdot R^{0.8}$

$L_p - L_w + 10 \log \dfrac{L}{\mu}$

dB

63

LEGEND

curve A : no side street for all R (Intensity Averaging)
curve A′ : no side street for R= ·1 (Exact Solution)
curve B : 1 side street for all R (Intensity Averaging)
curve B′ : 1 side street for R= ·9 (Exact Solution)

μx

Fig. 26 Intensity Averaging and Discrete Image Source
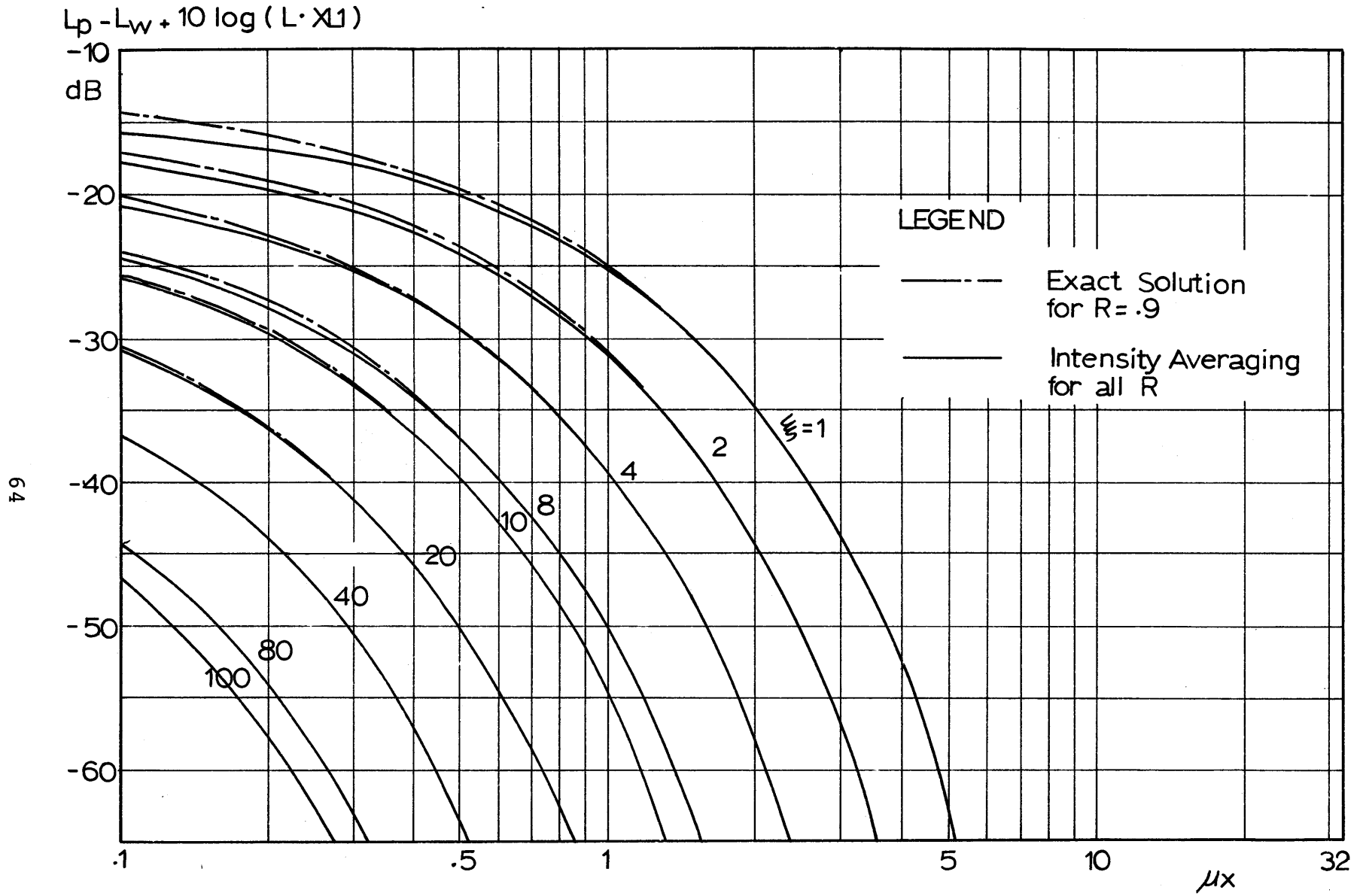
Fig. 27 Comparison of I. A. M. and D. I. S. for the First Side Street

$L_p - L_w + 10 \log (L \cdot X1)$

LEGEND

— · — Exact Solution for R = .9

——— Intensity Averaging for all R

$\xi = 1$

2. The nomogram for estimating L_p in Streets

Combining all the results so far, it is possible to draw a nomogram (Fig. 28) which can be used to estimate the sound pressure level in urban environments such as shown in Fig. 2.

The curves which represent straight streets are almost accurate with maximum deviation of $\pm$ 1 dB. The accuracy increases as R and μx increases. The curves which represent the first side street are reliable with deviation of $\pm$ 1 dB only beyond the receiver point at about one street width from the entrance of the side street. Likewise, the accuracy increases as R and ξ increases.
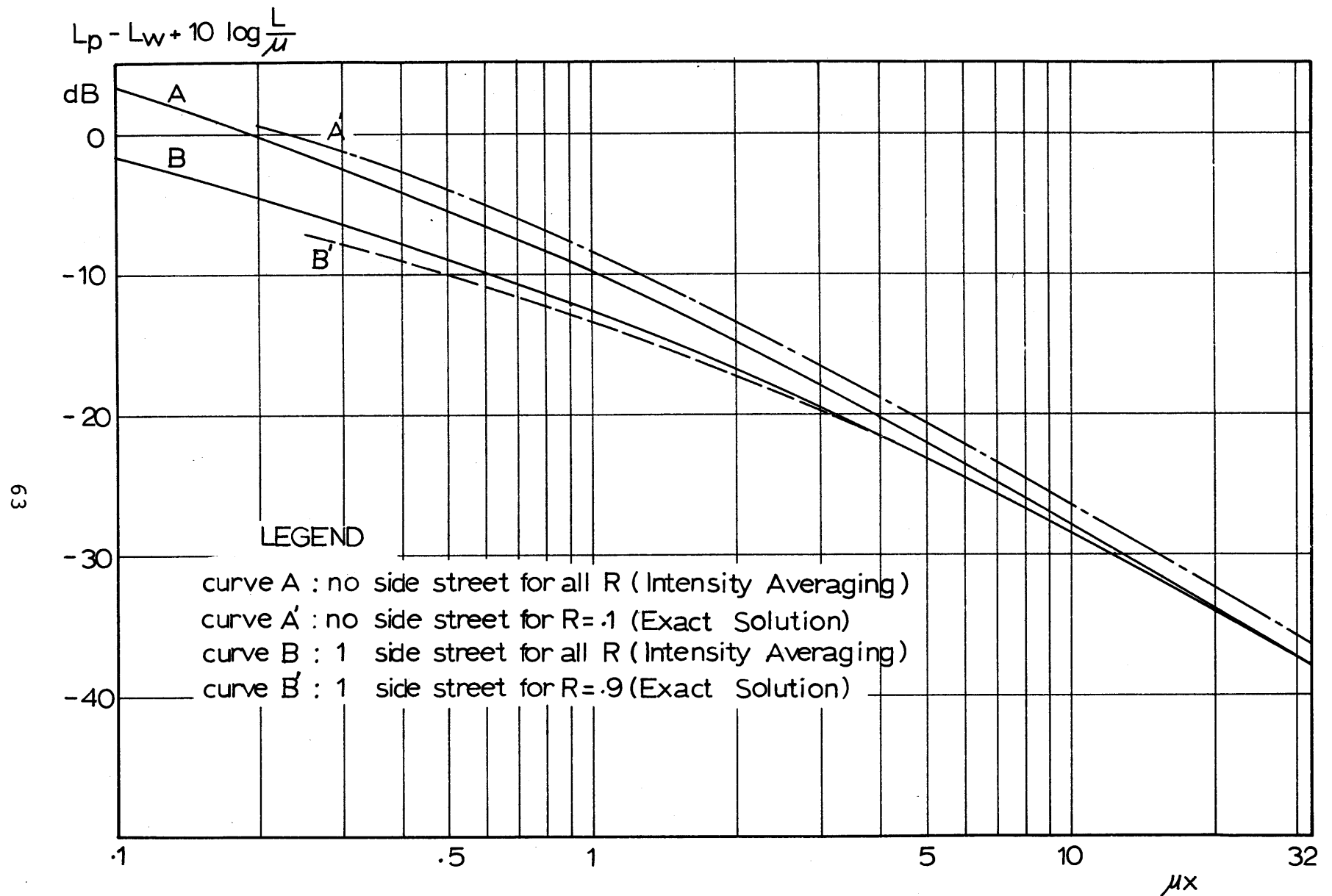
In Fig. 28 , the curves labelled A, B, C, D represent the sound level of the straight streets with 0, 1, 2, or 3 side streets respectively, and the curves numbered .1, .2, etc., represent the sound level in the first side street. The scale at the left hand side is for the straight streets, and the scale at the right hand side is for the first side street.

To explain how to use this nomogram, let us take an example of estimating L_p at the receiver positions 1, 2, 3, 4, or 5 in Fig. 2 , for given source power L_w , intensity absorption coefficient R, and dimensions such as L, XL1, XL2, etc. Then, μ and α can be calculated from equations (2), (32).

$$\alpha = \frac{2\cdot 81\,(1-R)}{\mu^2\,(1+R)}$$

$$\beta = L\cdot XL1\cdot R^{0.8}$$
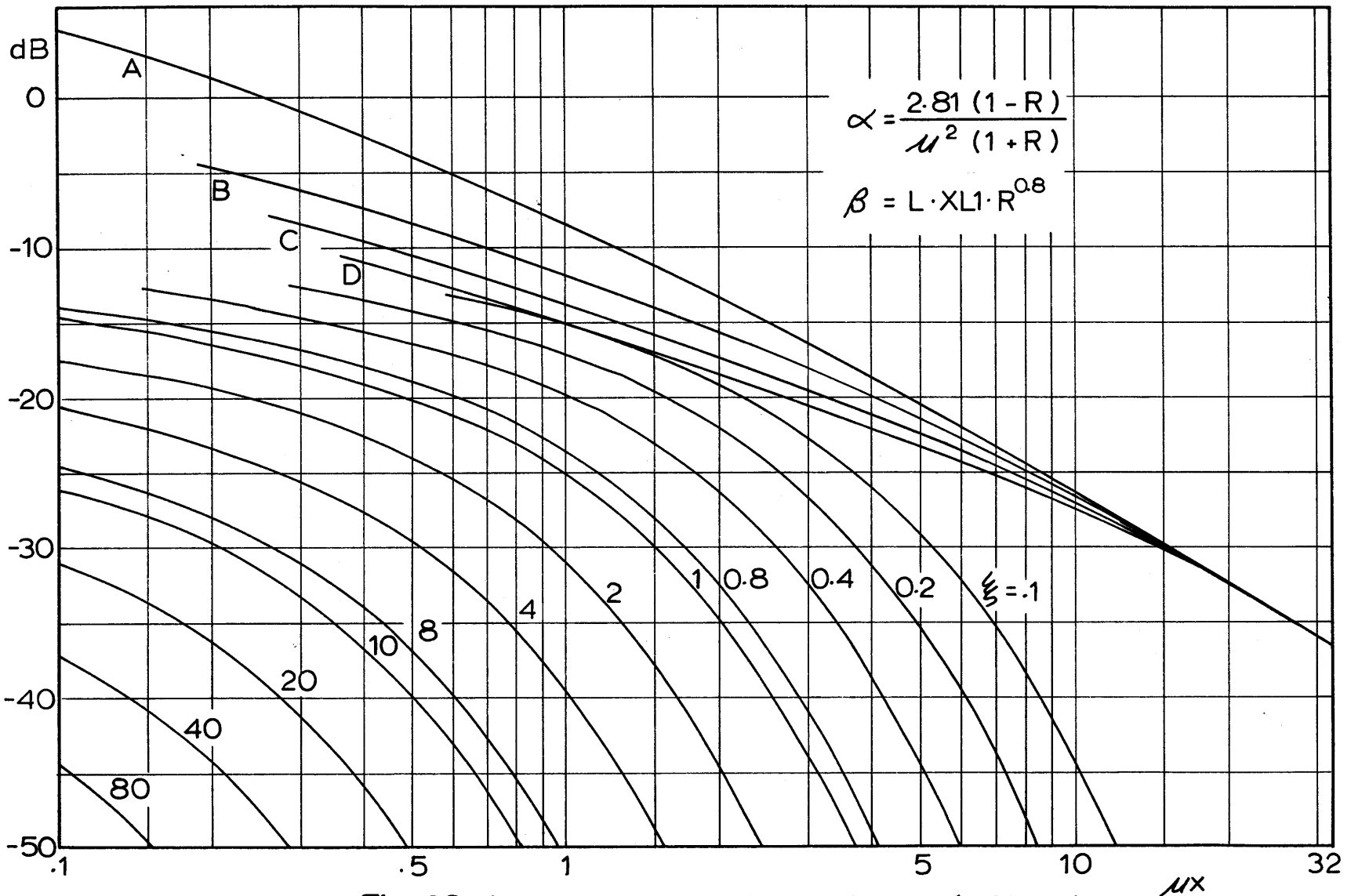
Fig. 28 Nomogram for Estimating L_p in Streets

$$\mu \ = \ \frac{-\ln R}{L}$$

$$\alpha \ = \ \frac{2.81 \ (1 - R)}{\mu^2 \ (1 + R)}$$

L_p can be obtained for receiver positions 1, 2, 3, or 4 from the relation

$$L_p \ = \ y_i + L_w - 10 \log \alpha$$

By substituting y_1, y_2, y_3, y_4, respectively.

Above y_i's were decided by the intersections of the curves A, B, C, D with $x = \mu x_1$, μx_2, μx_3, μx_4, respectively as shown in Fig. 29 , using the left hand side scale.

To get L_p at position 5 in Fig. 2 , get the intersection point of the curve $\xi = \frac{z}{XL1}$, with the line $x = \mu \ XL1$, where z is the distance from the centerline of the straight street to the receiver. Read the level y of that intersecting point using the right hand side scale. Then L_p at position 5 is given by

$$L_p \ = \ y_5 + L_w - 10 \log (XL1 \ L \ R^{0.8}).$$

μL

μL

μL

A

B

C

D

y_1

y_2

y_3

y_4

y_5

$\xi = z_5 / XL1$

μx_1 $\mu XL1$ μx_2 $\mu XL2$ μx_3 $\mu XL3$ μx_4
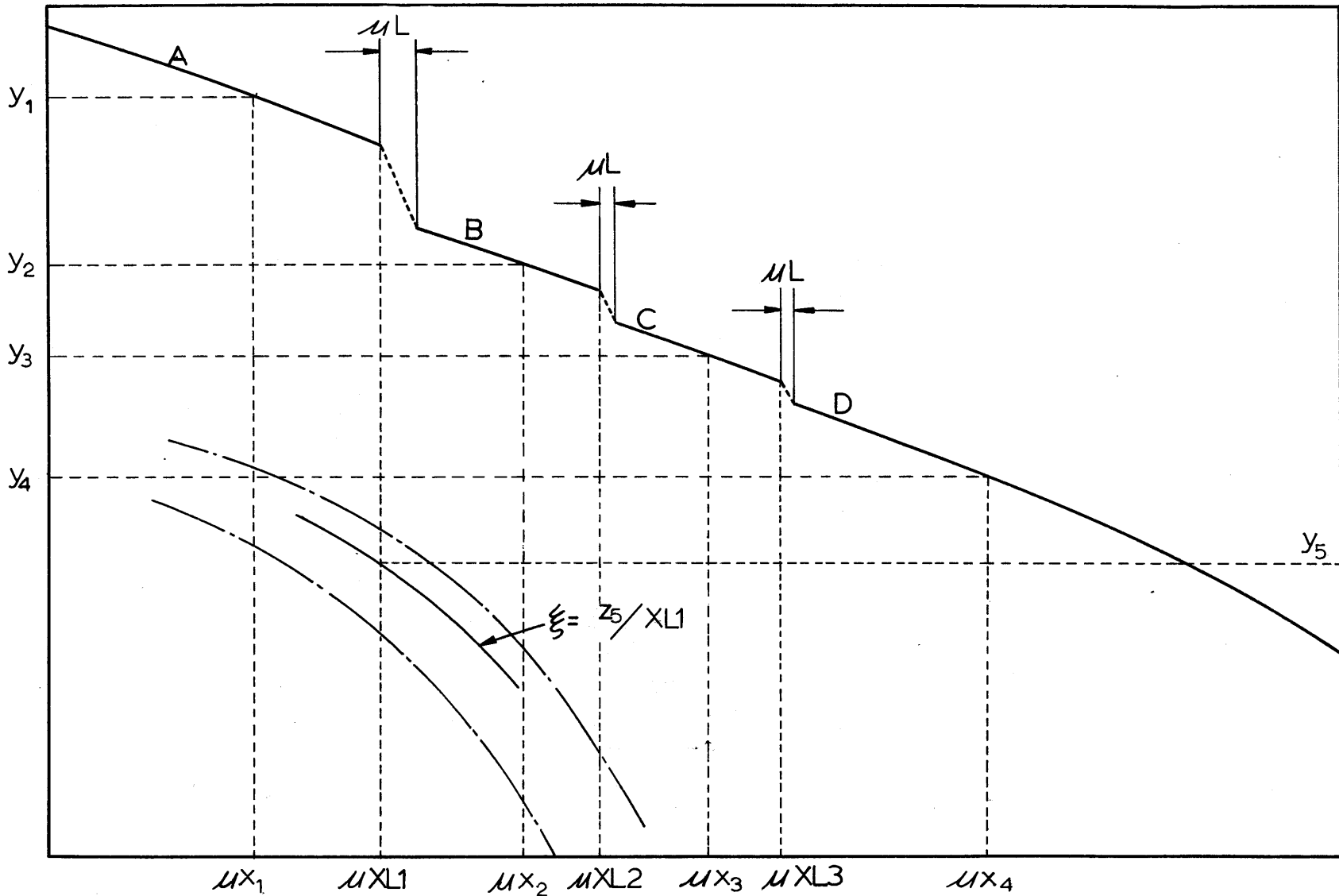
Fig. 29 Example of the Usage of the Nomogram

IV. GROUND EFFECT

Up to this point, the reflection from the ground has been neglected. Since most pavements have low absorption coefficient (.1 ∼ .3) the reflected waves may have a significant influence on the total sound pressure due to the interference with directly propagated sound waves.

A basic understanding can be gained by considering the model shown in Figure 30 .
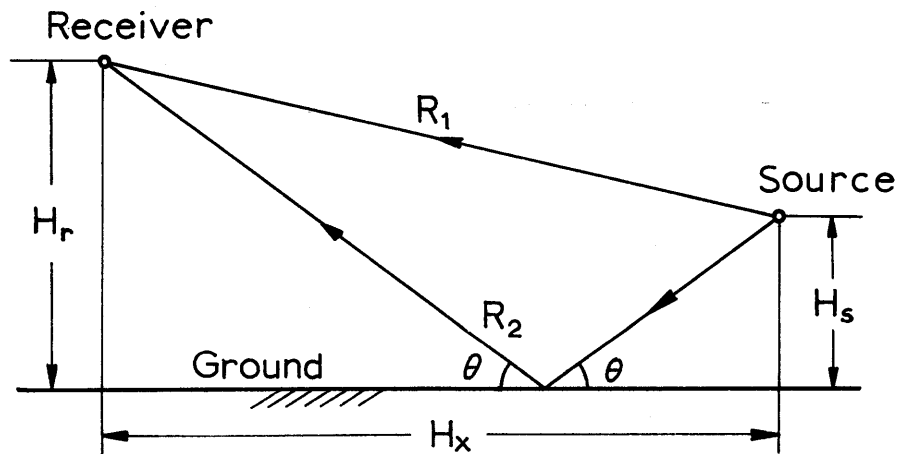
Fig. 30 Reflection from Ground

Here a point source is located H_s above the ground, separated by H_x horizontally from the receiver which is located H_r above

the ground. The ground has a pressure reflection coefficient for the angle of incidence θ, of magnitude r, and phase ψ.

The direct path R_1 and the reflected path R_2 can be expressed from geometry.

$$R_1 = [(H_r - H_s)^2 + H_x^2]^{\frac{1}{2}} \tag{1}$$

$$R_2 = [R_1^2 + 4 H_r H_s]^{\frac{1}{2}} \tag{2}$$

The sound pressure measured at the receiver point is a combination of the direct waves travelling R_1, and the reflected waves travelling R_2. These two sound pressures are given by,

$$P_1 = P \cos \omega t \tag{3}$$

$$P_2 = r P \frac{R_1}{R_2} \cos (\omega t + \phi_1) \tag{4}$$

where $\quad \phi_1 = \dfrac{10}{c} (R_2 - R_1) + \psi$

$\quad\quad c$ = speed of sound.

The mean square pressure at the receiver position is given by the mean square of the sum of P_1 and P_2. Thus,

$$P_3^2 = (P_1 + P_2)^2 = P_1^2 + P_2^2 + 2 P_1 P_2 \tag{5}$$

If the source is broadband, equation (5) has to be integrated [19] over the frequency range we are interested in. Thus,

$$P^2_{\Delta f} = \frac{P^2}{2} [1 + (r \frac{R_1}{R_2})^2 + 2 r \frac{R_1}{R_2} \frac{\cos \phi_2 \sin \phi_3}{\phi_3}] \qquad (6)$$

where

$$\phi_2 = \pi(f_2 + f_1) \gamma$$

$$\phi_3 = \pi(f_2 - f_1) \gamma$$

$$\gamma = (R_2 - R_1)/c$$

$$\frac{P^2}{2} = P^2_{rms}$$

Going back to the street problem, it is now simple to include the ground effect if equation (6) is used in calculating sound pressure for each image source, S_1, S_2, S_2', S_3, S_3', ... For example, take one of the image sources, S_i in Fig.   . The mean square pressure, averaged over street width L, is given by

$$< P^2_{rms} > = c \frac{W}{4\pi L} \int_{-L/2}^{L/2} \frac{R^{i-1} \, dy}{x^2 + [(i - 1)L + y]^2} \qquad (7)$$

If ground reflection is included, using equation (6), the averaged mean square pressure at the receiver position due to
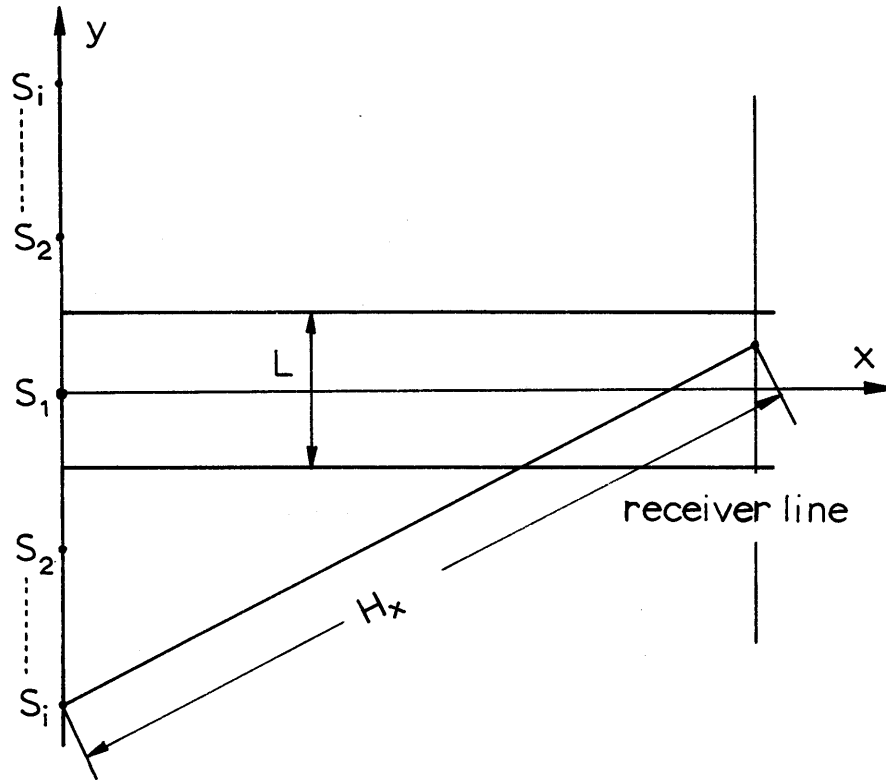
Fig. 31 Application of Ground Effect to an Image Source

i^{th} image source for the frequency range f_1 to f_2 can be written as follows.

$$< P^2_{rms} >_{\Delta f} = \rho c \; \frac{W}{4\pi L} \int_{-L/2}^{L/2} \frac{R^{i-1} \; (1+(r \frac{R_1}{R_2}) + 2r \; \frac{R_1}{R_2} \; \frac{\cos \phi_2 \; \sin \phi_3}{\phi_3}) \; dy}{x^2 + [(i - 1)L + y]^2}$$

(8)

72

$$L_p = 10 \log \left[\frac{1}{f_{max} - f_{min}} \sum_j \sum_i \text{antilog}\{(10 \log P_{ij} \right.$$

$$\left. + \text{A-weighting})/10\} \Delta f_j \right] - 10 \log P_{ref}^2 \qquad (9)$$

where $\quad P_{ref} = 2 \times 10^{-5} \text{ N/m}^2.$

The index i denotes the position of the image source, j denotes a third octave frequency band we are interested in.

P_{ij} is the mean square pressure averaged over street width L at the receiver position due to the ith image source and j^{th} frequency band.

Before going through complicated computations, let us take a look at equation (6) to get a rough idea about how much the resulting pressure will differ from the sound pressure without ground reflection.

As H_x , the horizontal distance between source and receiver, increases, in the limit, the path difference $R_2 - R_1$ approaches zero from equation (1), (2). In that case, equation (6) becomes,

$$P_{\Delta f}^2 = \frac{P^2}{2} (1 + r)^2 \qquad (10)$$

Choosing intensity absorption coefficient $\alpha_A \cong 0.2$ which is the case of asphalt pavement [19], the pressure reflection

The actual computation is carried out in the frequency range from 89.1 to 8913 using one third octave bands. For each band width, equation (8) is computed, converted into sound level, and A-weighted [23] according to the center frequency of the one third octave band considered. (Fig. 32).
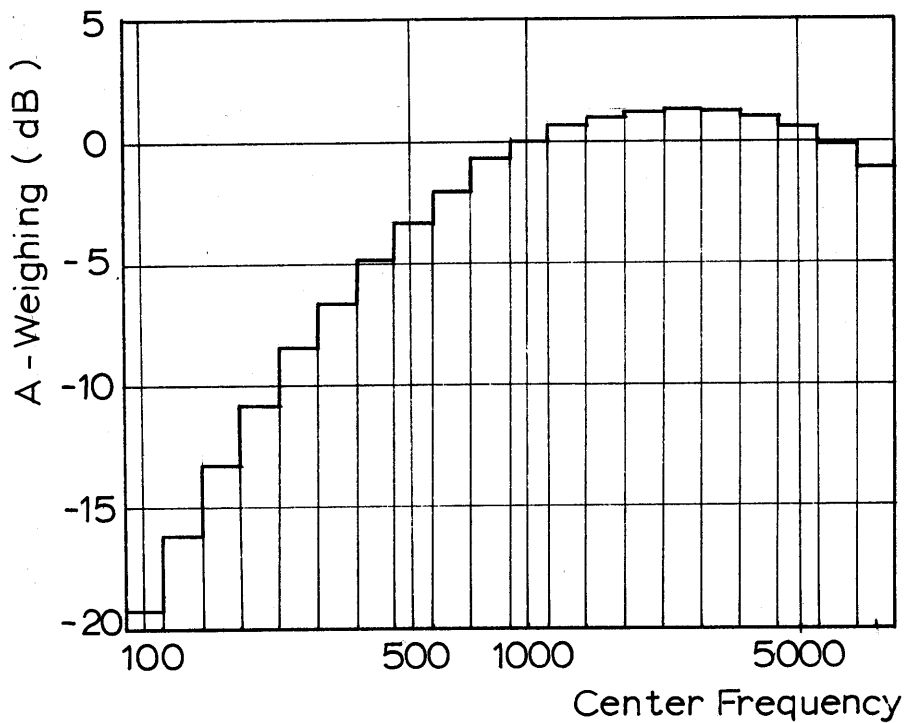

Fig. 32   A-Weighting in One Third Octave Band

Therefore, the resulting sound pressure level due to the whole image sources through the entire frequency range can be written as follows.

coefficient r is given by

$$r = \sqrt{1 - \alpha_A} \simeq 0.9$$

Substituting $r \simeq .9$ into equation (10), we can predict that
in the straight street paved with asphalt, we would see about
5.6 dB increase above the sound pressure level without ground
reflection at the very far distance from the source.

In Fig. 33, the cases of $H_r = H_s = 1.5$ meters,
$R = 0.1, 0.5, 0.9$, $L = 15, 30$ meters are plotted in comparison
with the case of no ground reflection. In Fig. 34, the
difference ΔL_p due to the ground reflection is plotted using
the actual distance scale for various cases mentioned above.

As shown in Fig. 34, the increase in sound pressure
level ΔL_p does not depend on the value of R, or the width of
the street L, but depends only on the distance from the source
to the receiver for a given source strength and r.

In the very near region (within .5 meters from the
source), ΔL_p is less than .5 dB down to 0 dB in the limit.
In the region from about 2 meters to 200 meters, ΔL_p is
approximately 2.5 dB. There is a transition region from
about 200 meters to 1000 meters in which ΔL_p increases
gradually up to 5.6 dB. Beyond this transition region, ΔL_p
remains constant at 5.6 dB which was predicted by equation (10).
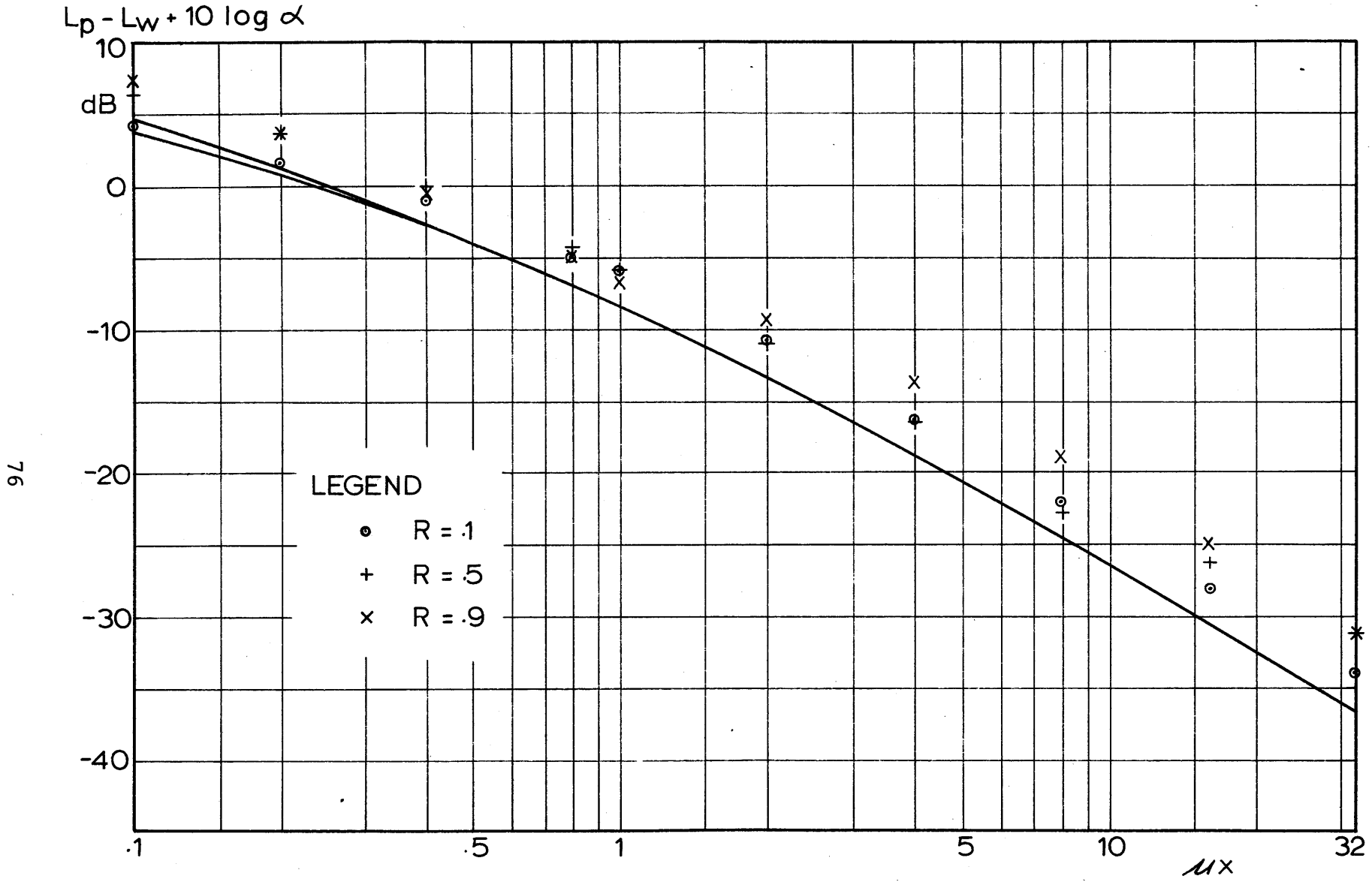
Fig. 33 Comparison of L_p in Straight Street with and without Ground Effect

The vertical axis is labeled $L_p - L_w + 10 \log \alpha$ (dB), the horizontal axis is labeled μx.

LEGEND

⊙ $R = .1$

+ $R = .5$

× $R = .9$
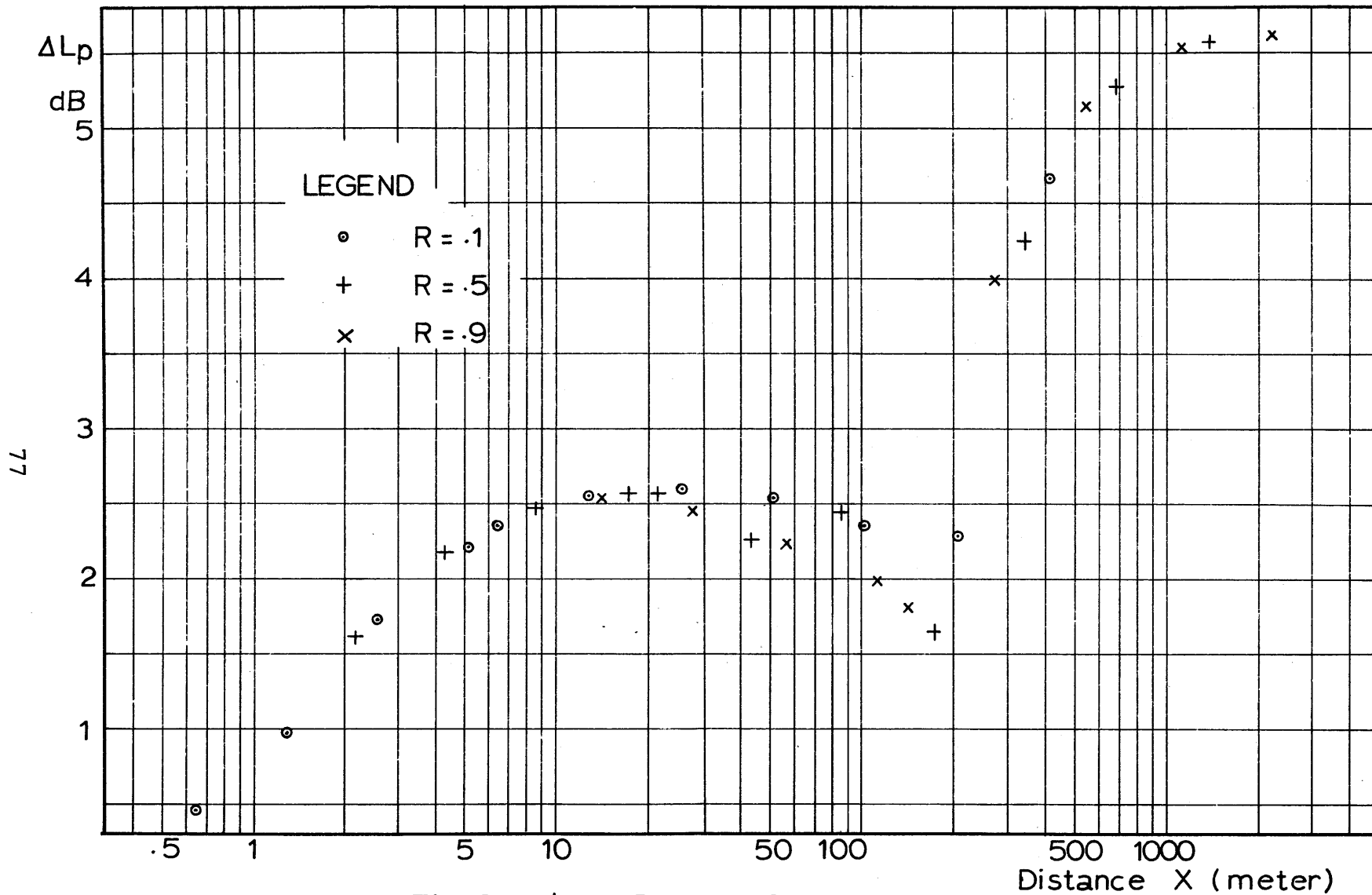
Fig. 34 ΔLp Due to Ground Effect

If we neglect the sound pressure level which is 20 dB below the level at the unit distance from the source, we can safely say that the increase in sound pressure level due the ground reflection is approximately 2.5 dB, since beyond 200 meters away from the source, the sound pressure level is already below 20 dB from the above reference level in most cases of straight street propagation. The same argument will hold for the side street cases as well. Therefore, for practical purposes, 2.5 dB increase in sound pressure level would be a good approximation in the region of our interest.

V. CONCLUSIONS AND RECOMMENDATIONS

Sound propagation in urban streets has been investigated using a simplified model which consists of buildings, that have rectangular cross sections and non-reacting surfaces with the intensity reflection coefficient R, and streets of a uniform width. The ground effect was neglected at first for simplicity, but was included later.

In the low frequency region where a plane wave was assumed to be incident on our model, an analytic solution was obtained for N layers of buildings, which is an extension of the study done by Kristiansen and Fahy [9]. For the N = 1 case, interesting results were obtained. By assuming the acoustic input impedance of a side branch, Z_s, to be equal to $\rho_0 c/S$, it was possible to estimate the insertion loss of 6 dB for propagation through an intersection at low frequencies.

In the high frequency region, which is deemed to be more relevant to explain the actual situation in street propagation, in that the wavelength is usually much smaller than the street width, a point monopole source was located inside a street to find the sound field down the straight street and side streets.

A general purpose computer program was developed to be used for the straight street with N side streets and also for the Nth side street where N = 0, 1, 2, ...

In order to find suitable non-dimensional variables which will properly explain the sound propagation phenomena in streets, the average across the street width of the sound intensity was evaluated. This method is applicable to the side street as well as the straight street propagation.

In addition, for the straight street with no side streets, the incoherent varying strength line source approximation was used as in Schlatter [1] to replace the image sources produced by the reflections from the building surfaces.

By combining the results of the above line source approximation and the intensity averaging method, the desired two non-dimensional variables were obtained. Using the variables, it was possible to draw a single curve shown in Fig. 18 , from the data obtained by the computer solution, which explains the general cases of straight street with no side streets. In the same way, it was also possible to get a single curve for the case of a straight street with one side street. As a natural extension, it was found that we can use the same non-dimensional variables to explain the straight street propagation with an arbitrary number of side streets. (Fig. 21)

For the first side street propagation, using the result of the intensity averaging method, it was possible to obtain three non-dimensional variables, which enabled us to draw a set of curves that can be used to estimate the sound level down the side street.

Combining all the results above, a nomogram to estimate the sound level down the streets was presented in Fig. 28 .

Finally, the neglected ground effect was investigated. The ground was assumed to be smooth, flat, and non-reacting with absorption coefficient $\alpha = .2$ which is approximately the case of asphalt pavement. An A-weighted white noise was used in the frequency range of 100 to 8000 in terms of the center frequency of the one third octave band.

From the analysis of the computer solution, it was observed that the ground effect is approximately independent of the intensity reflection coefficient of the buildings, R, or the width of the street. It depends, however, on the pressure reflection coefficient of the ground and the distance from the source to the receiver for a given source power. The increase in sound level due to the ground, ΔL_p, is shown in Fig. 34.

It is now possible to estimate the sound level L_p down the straight streets with N side streets, and down the first side street by adding the appropriate value of ΔL_p from Fig. 34 , to the L_p obtained from the nomogram.

As an extension of this study, the following are recommended: (1) obtaining the nomogram for the Nth side street when $N \geqq 2.$, (2) the inclusion of the surface roughness of buildings and the ground, and the influence of the scattering by trees or other obstacles in streets, and (3) the inclusion of the meteorological factors.

81

The elements f, g, f', g', of the transfer matrix can be obtained by

$$\begin{vmatrix} f & g \\ f' & g' \end{vmatrix} = \begin{vmatrix} a & b \\ a' & b' \end{vmatrix}^{N-1}$$

where $\begin{vmatrix} a & b \\ a' & b' \end{vmatrix}$ is the transfer matrix for each two adjacent columns of scatterers, i.e.

$$\begin{vmatrix} A'' \\ B'' \end{vmatrix} = \begin{vmatrix} a & b \\ a' & b' \end{vmatrix} \begin{vmatrix} A \\ B \end{vmatrix}$$

The elements a, b, a', b' can be expressed up to $O(kd)$, $O(kh_1)$ as

$$a = e^{-jkh} [1 - G \frac{h_1}{d} + jkh_1 (1 - G \frac{h_1}{d})]$$

$$a' = a - 1 - jkh_1$$

$$b = - e^{jkh} G \frac{h_1}{d} [1 - jkd (\frac{1}{2G})]$$

$$b' = b + 1 + jkh_1$$

$$G = (e^{j\ell\alpha_o} + e^{-j\ell k})(e^{j\ell\alpha_o} - e^{j\ell k})/(e^{j\ell k} - e^{-j\ell k})$$

The coefficients of equations (10), (11) are given by

$$g_1 = \frac{e^{-jkh}(f + g) + e^{jkh}(f' + g')}{2(fg' - f'g)}$$

$$g_2 = \frac{- e^{-jkh}(f + g) - e^{jkh}(f' + g')}{2(fg' - f'g)}$$

$$g_3 = \frac{e^{-jkh}(g - f) + e^{jkh}(g' - f')}{2(fg' - f'g)}$$

$$g_4 = \frac{e^{-jkh}(g - f) - e^{jkh}(g' - f')}{2(fg' - f'g)}$$

REFERENCES

1. Schlatter, W.R., "Sound Power Measurement in a Semi-Confined Space," M.Sc. Thesis, M.I.T., Cambridge, Mass. July 1971.

2. Davies, H.G., "Noise Propagation in Corridors," J. Acoustical Society of America, Vol. 53, No. 5, 1973.

3. Wiener, F.M., Malme, C.I., and Gogos, C.M., "Sound Propagation in Urban Areas," J. Acoustical Society of America, Vol. 37, No. 4, 1965.

4. Delaney, M.E., Copeland, W.C., and Payne, R.C., "Propagation of Traffic Noise in Typical Urban Situations," NPL Acoustic Report No. AC 54, Oct. 1971.

5. Delaney, M.E., Rennie, A.J., and Collins, K.M., "Scale Model Investigations of Traffic Noise Propagation," NPL Acoustic Report No. AC 58, Sept. 1972.

6. Donovan, P.R., "Model Study of the Propagation of Sound from V/STOL Aircraft into Urban Environs," M.Sc. Thesis, M.I.T., Cambridge, Mass. 1973.

7. Holmes, D.G., and Lyon, R.H., "A Numerical Model of Sound Propagation in Urban Areas," M.I.T., Cambridge, Mass. 1974.

8. Fishman, G.S., Concepts and Methods in Discrete Event Digital Simulation, John Wiley, N.Y., 1973.

9. Kristiansen, U.R., and Fahy, I.J., "Scattering of Acoustic Waves by an N-layer Periodic Grating," J. Sound and Vibration, Vol. 24, No. 3, 315-335, 1972.

10. Shenderov, E.L., "Sound Diffraction by Slits in a Plate of Finite Thickness," Soviet-Physics Acoustics, Vol. 10, No. 3, Jan. - Mar., 1965.

11. Pande, L., "Model Study of Aircraft Noise Reverberation in a City Street," Interim Report, DOT-TSC-93, Dept. of Mech. Eng., M.I.T., April 1972.

12. Kinney, W.A., "Helicopter Noise Experiment in an Urban Environment," M.Sc. Thesis, M.I.T., Cambridge, Mass., 1973.

13. Tocci, G.C., "Noise Propagation in Corridors," M. Sc. Thesis, M.I.T., Cambridge, Mass., 1973.

14. Morse, P.M., and Ingard, K.U., Theoretical Acoustics, McGraw-Hill Book Co., 1968, pp. 366-369.

15. Moore, C.J., "A Solution to the Problem of Measuring the Sound Field of a Source in the Presence of a Ground Surface," J. Sound and Vibration, Vol. 16, No. 2, 269-282, 1971.

16. Delaney, M.E., Bazely, E.N., "A Note on The Effect of Ground Absorption in the Measurement of Aircraft Noise," J. Sound and Vibration, Vol. 16, No. 3, 315-322, 1971.

17. Piercy, J.E., and Embleton, T.F.W., "Effect of Ground on Near - Horizontal Sound Propagation," Society of Automotive Engineers, Automotive Engineering Congress Paper No. 740211, 1974.

18. Sutherland, L.C., "Sound Propagation in Open Terrain From a Source Near the Ground," J. Acoustical Society of America, Vol. 53, p. 339, 1973.

19. Bettis, R.A., and Sexton, M.Z., "The Effect of Test Site Topography in Vehicle Noise Measurement," General Motors Proving Ground Report prepared for the 85th Meeting of Acoustical Society of America, April 1973.

20. Whittaker, E.T., and Watson, G.N., A Course of Modern Analysis. 4th Edition, Cambridge University Press, 1958.

21. Morse, P.M., and Feshbach, H., Methods of Theoretical Physics, McGraw-Hill Book Co., pp. 1430-1432, 1953.

22. Beckmann, P., and Spizzichino, A., The Scattering of Electro Magnetic Waves from Rough Surfaces, International Series of Monographs on Electromagnetic Waves, Vol. 4.

23. Beranek, L.L., Noise and Vibration Control, McGraw-Hill Book Co., pp. 77-79, 1971.